

# Nuclear Moment of Inertia at High Spin\*

Raymond A. Sorensen

Carnegie-Mellon University, Pittsburgh, Pennsylvania 15213

The moment of inertia  $\mathcal{J}$  of deformed nuclei increases with increasing angular momentum  $I$  in the ground-state rotational band. Recent energy measurements of rare-earth nuclei show that while the increase is smooth at low angular momenta, at about spin 14–16 in a number of nuclei there is a sudden substantial rise in the moment of inertia. In some cases  $\mathcal{J}$  rises faster than  $I$  so that the rotational frequency  $\omega = I/\mathcal{J}$  actually decreases with increasing  $I$  producing a characteristic backbending  $\mathcal{J}$  vs  $\omega$  curve. A singular behavior at about these spin values was predicted over ten years ago by Mottelson and Valatin as a Coriolis antipairing effect. The present article will discuss the experimental data and describe calculations of the nuclear moment of inertia. Calculations made both before and after the recent experiments will be considered.

## CONTENTS

I. Introduction.....	353
II. Phenomenological Description of the Data.....	355
A. The $\mathcal{J}$ vs $\omega^2$ Plot.....	356
B. The Data.....	359
III. Theoretical Descriptions.....	359
IV. The Cranking Model.....	360
A. The Pushing Model Result.....	361
B. Interpretation of the Cranking Formula.....	362
C. The Effect of Residual Interactions.....	363
D. Moment of Inertia with Pairing.....	363
E. The Mottelson-Valatin Effect (Basic Idea).....	364
F. Theory of Rotation.....	364
G. The Mottelson-Valatin Effect (Detailed Calculations).....	366
1. Perturbation Calculations for Low Spin States..	366
2. Calculations for High Spin States.....	367
3. The Shape of the Singular Behavior at High Spin.....	369
4. The S-Shaped Curves.....	370
5. Triaxial Nuclei.....	372
6. State-Dependent Energy Gap.....	372
V. Particle Plus Rotor Models.....	372
A. Krumlinde-Szymanski (KS) Calculation.....	372
B. Stephens-Simon (SS) Calculation.....	374
VI. Conclusions.....	375

## I. INTRODUCTION

During the last two years,  $E2$  gamma transitions have been observed in  $(\alpha, xn, \gamma)$  and heavy ion  $(HI, xn, \gamma)$  reactions from states as high as  $I=22+$  in deformed even-even nuclei. The pioneering work of Morinaga and co-workers (Morinaga and Gugelot, 1963; Morinaga and Lark, 1965; Lark and Morinaga, 1965) showed that a relatively clean spectrum corresponding to a stretched  $E2$  cascade down the ground-state rotational band could be obtained up to about the 10+ level.

Then Diamond and Stevens and co-workers in a series of papers (Diamond *et al.*, 1964, 1969; Stephens *et al.*, 1964, 1965; Ward *et al.*, 1967; Newton *et al.*, 1970; Nordhagen *et al.*, 1970) were able to push the top spin observed to about 18+ and in addition deduced many interesting properties of the ground band and the way it was fed at the top in the reactions. First, the observed energy spacing of the 0+, 2+, 4+, etc. members of the ground band increased less rapidly

than the form  $E_I = \hbar^2 I(I+1)/(2\mathcal{J})$  expected for a constant moment of inertia,  $\mathcal{J}$ . This was interpreted as some sort of centrifugal stretching causing the moment of inertia  $\mathcal{J}$  to increase smoothly with angular momentum up to the highest spins seen. As will be shown, it is now thought that Coriolis antipairing effects are more important in increasing  $\mathcal{J}$ .

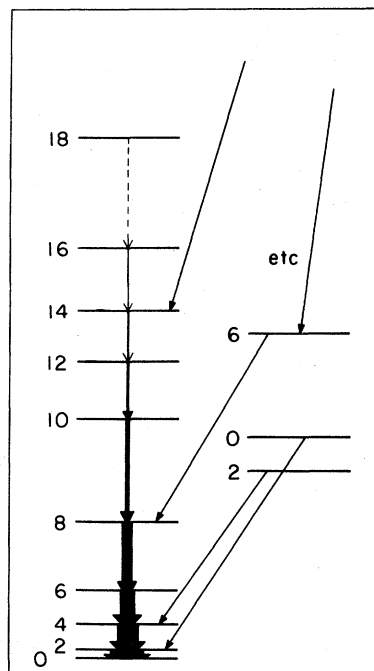


FIG. 1. Schematic level diagram. The thickness of the arrows indicate the observed gamma intensity.

Second, it was noted that even though the compound nucleus probably has  $I \gg 20$  after the capture of the  $\alpha$  particle or heavy ion and the neutron emission, nonetheless only  $\gamma$ 's from  $I \sim 18$  or lower were observed as lines. Thus the  $\gamma$ 's leading from the high starting spin down to  $I \sim 18$  must follow several tracks (5–10 tracks being enough so that individual lines would not

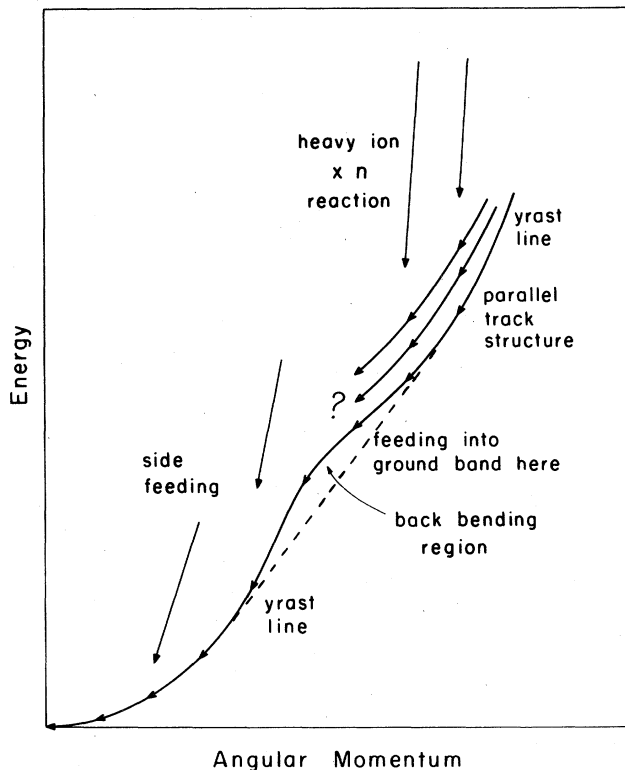


FIG. 2.  $E$  vs  $I$  plot for the level diagram of Fig. 1. That portion of the yrast line (lowest energy for each spin) which is concave downward corresponds to the "backbending" region in  $\theta$  vs  $\omega^2$  plots such as Figs. 5-9. The dashed curve could result from an unprojected cranking model calculation (see Sec. IVG4).

be seen); also there must be some selection rule keeping each nucleus in its track to avoid rapid decay to the yrast line (state of lowest energy at each spin). From  $I \sim 18$  to the  $0^+$  ground state, the main transitions observed are those down the ground-state rotational band with relatively little side feeding, as shown in Figs. 1 and 2. The lowest transitions of the band are thus strongest, with gradual weakening toward the higher spins, and then a rapid drop to invisibility about  $I \sim 18-20$ .

The entire cascade time (including the unseen  $\gamma$ 's) is fast, corresponding to enhanced  $E2$  transition rates, each of an energy corresponding to a smooth  $E$  vs  $I$  dependence. The yrast line (lowest energy state for each  $I$  value) must be a monotonically increasing function of  $I$  as no isomers are seen. If, for example, the lowest  $I=16$  state lay below the lowest  $I=13, 14, 15$  states, it could decay only by  $E4$  transition and would thus have a long enough lifetime to be observed as a time-delayed isomer.

The recent measurements, first from Stockholm (Johnson 1971, 1972), and subsequently from other places (Buescher *et al.*, 1972; Lieder *et al.*, 1972; Sunyar *et al.*, 1972; Thieberger *et al.*, 1972; Warner

*et al.*, 1972) study in detail the weak transitions at the top of the ground-state rotational band. By the use of (a)  $\gamma\gamma$  time coincident spectra, (b) angular distributions, and (c) excitation functions, it has been possible to assign uniquely each observed line to a definite transition  $I, I-2$  as high as  $I=22$  in one case.

The three techniques mentioned above use the facts that:

(a) All transitions in time coincidence with the  $I_0, I_0-2$  line and having smaller  $I$  must have the  $I_0$  state as a parent and thus will have the same intensity (aside from the energy dependence of instrument sensitivity). The feeding into the band may occur at any  $I > I_0$  so that these higher transitions will fall in intensity in the same fashion as in a singles spectrum taken from either one of the two  $\gamma$  detectors alone.

(b) The nucleus following ( $HI, xn$ ) is aligned and the alignment decreases in time as the  $\gamma$ 's go down the band, giving the lower transitions more constant angular distributions than the higher ones.

(c) Higher incident  $HI$  energy increases the initial average angular momentum and thus pushes the side feeding higher up the band causing a measurable change in the intensity ratios of the  $\gamma$ 's.

Figure 3 shows the singles spectrum in  $^{162}\text{Er}$  of Johnson *et al.*, in which it is seen that the 18, 16 and 16, 14 transitions lie below the 12, 10 transition. Transitions corresponding to higher spins are weaker. The corresponding time coincident spectra are shown in Fig. 4 in which it is seen that transitions for spins below the gate are of equal intensity while those above are weakened as in the singles spectrum. The sequence of the transitions is uniquely determined by this measurement.

The  $\gamma$  intensities were measured for 39- and 41-MeV  $\alpha$  particles incident on  $^{161}\text{Dy}$ . The higher energy spectrum has a changed  $\gamma$  intensity ratio with the  $\gamma$ 's assigned as coming from higher up the band having the greater intensity increase. This confirms the assignment of spins.

Finally, the angular distribution of each line is measured relative to the incident  $\alpha$  direction with the result that the characteristic  $E2$  shape is found with the strongest angular distribution observed at the top of the band, with gradual smoothing for the transitions lower down corresponding to the gradual loss of alignment.

By these methods unique spin assignments can be made. It is also clear that at least at these high spins, a spin assignment based on the regularity of energy spacing is completely invalid.

The result of these measurements is that, for a number of rare-earth nuclei, the weak transitions near the top of the observed band do not increase smoothly in energy with increasing  $I$  (corresponding to a constant

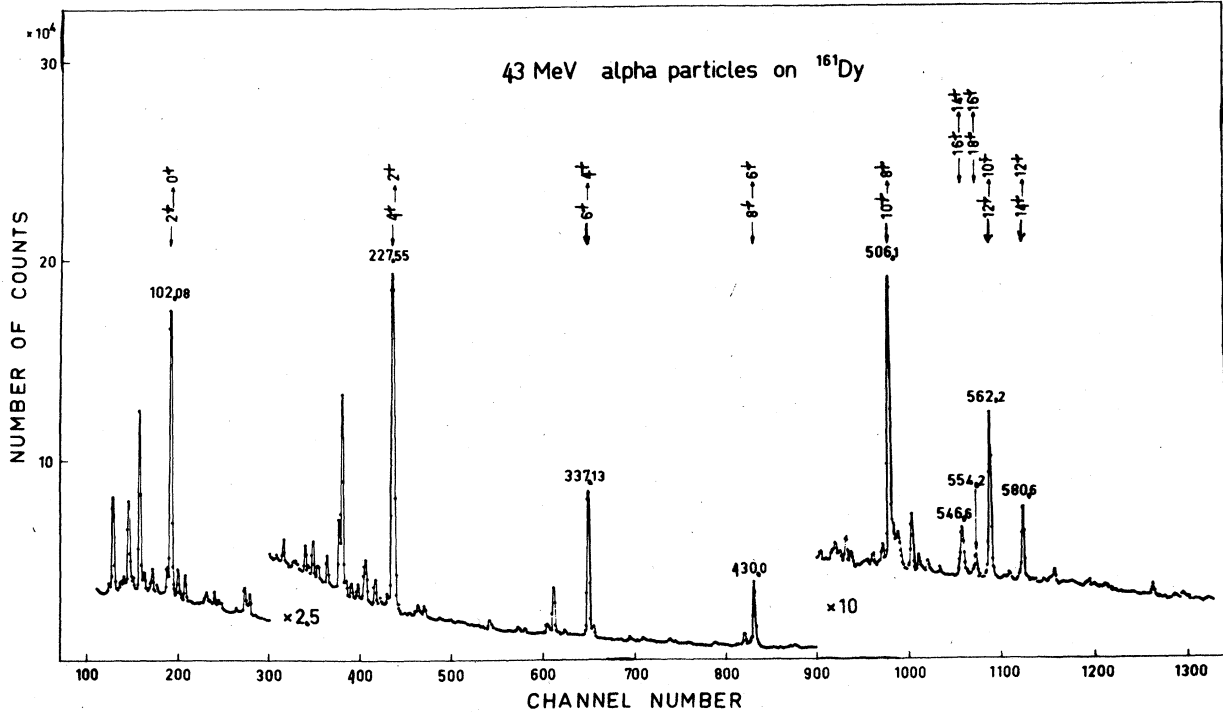


FIG. 3. Singles gamma-ray spectrum with transitions assigned to the ground state band in  $^{162}\text{Er}$ . The  $I=20$  to  $I=18$  transition has now also been identified as shown on Fig. 6(a) (Sunyar, 1972). [Taken from Johnson *et al.* (1972)].

or slowly increasing moment of inertia,  $\mathcal{J}$ ), but may be very close to each other in energy or even momentarily decrease in energy with increasing  $I$  corresponding to a very rapidly increasing moment of inertia at about spin 14–16. The effect can be dramatic, corresponding to a near doubling of the moment of inertia over a spin change interval of only 4–6 $\hbar$  units.

This sudden increase in  $\mathcal{J}$  was ascribed to the Mottelson–Valatin Coriolis antiparing effect (the CAP effect) (Mottelson and Valatin, 1960). It is the purpose of this article to present the background for descriptions of nuclear rotation, and to review both the detailed calculations which were made before the recent experimental results, and the calculations motivated by these results.

## II. PHENOMENOLOGICAL DESCRIPTION OF THE DATA

The observed quantity is the transition energy  $\Delta E_{I,(I-2)}$  for each even  $I$  value. For a perfect rotor we have

$$E_I = \hbar^2 I(I+1) / (2\mathcal{J}) = \hat{I}^2 / (2\mathcal{J}) \quad (1)$$

so that

$$\Delta E_{I,(I-2)} = \hbar^2 (2I-1) / \mathcal{J}. \quad (2)$$

For the deviations from this behavior, the form first

suggested was an expansion

$$E_I = AI(I+1) + B[I(I+1)]^2 + C[I(I+1)]^3. \quad (3)$$

It is well known that convergence is poor for this form, even for low spins. That is, if  $A$  and  $B$  are chosen from  $\Delta E_{2,0}$  and  $\Delta E_{4,2}$  and  $C=0$ , Eq. (3) is valid only through about  $\Delta E_{6,4}$ . The inclusion of  $C$  makes Eq. (3) reasonable only to about  $\Delta E_{10,8}$ .

The work of Harris (1965) and later the variable moment of inertia (VMI) model of Mariscotti, Scharff-Goldhaber, and Buck (1969) suggested an expansion in powers of the square of the angular velocity of rotation  $\omega$  instead of the angular momentum  $I$ . Classically,  $I$  and  $\omega$  are continuous variables with the relation

$$I = \mathcal{J}\omega \quad (4)$$

and Hamilton's equation relates  $\omega$  to the energy by

$$dE/dI = \omega. \quad (5)$$

Observe that if the derivative in Eq. (5) is approximated by  $\Delta E_{I,(I-2)} / (2\hbar)$ , the rotation frequency  $\omega$  is just half the frequency of the emitted  $\gamma$  ray, as would be expected for a deformed nucleus with reflection symmetry such that a rotation through  $\pi$  degrees brings the system back to its initial shape. Equation (5) is clearly satisfied for the perfect rotor Eq. (1).

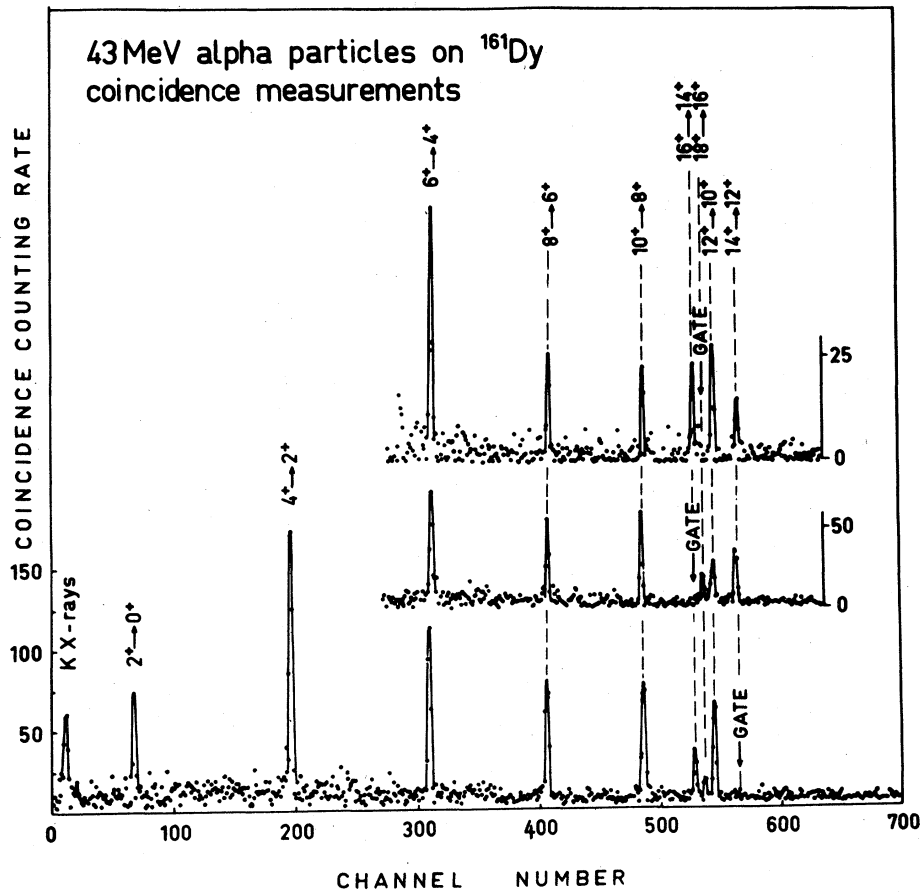


FIG. 4. Coincidence spectra in  $^{161}\text{Dy}$  [from Johnson *et al.* (1972)]. The plot shows counts in close time coincidence (about 90 nsec) with a count in the channel marked as gate.

If  $\mathcal{I}$  is not held constant, but may depend on some parameters (e.g., deformation and pairing parameters) indicated by  $\Delta$ , the energy is

$$E_I = I^2 / [2\mathcal{I}(\Delta)] + V(\Delta), \quad (6)$$

where  $V(\Delta)$  is an intrinsic energy. Equation (6) is to be minimized at fixed  $I$  to determine  $\mathcal{I}$  and  $V$ . Thus Eq. (5) still follows, and furthermore

$$dV/dI = \frac{1}{2}\omega^2 (d\mathcal{I}/dI), \quad (7)$$

so that

$$\omega^2 = 2dV/d\mathcal{I}. \quad (8)$$

The two-parameter variable moment of inertia (VMI) model, which is highly successful up to about  $I \sim 14$  in many cases, uses a specific dependence of the intrinsic energy  $V$  on  $\mathcal{I}$ , namely:

$$V(\mathcal{I}) = V_0 + (8C)^{-1}(\mathcal{I} - \mathcal{I}_0)^2 \quad (9)$$

so that Eq. (8) gives

$$\mathcal{I} = \mathcal{I}_0 + 2C\omega^2, \quad (10)$$

a simple linear dependence of the moment of inertia on angular velocity squared. An equivalent result is obtained by keeping just two terms in the Harris ex-

pansions:

$$E = \frac{1}{2}\omega^2(\mathcal{I}_0 + 3C\omega^2 + 5D\omega^4 + \dots) \quad (11)$$

$$I = \omega\mathcal{I} = \omega(\mathcal{I}_0 + 2C\omega^2 + 3D\omega^4 + \dots) \quad (12)$$

which also satisfy Eq. (5). The model is completed by the substitution  $I \rightarrow [I(I+1)]^{1/2}$ . Thus two terms in the  $\omega^2$  expansion of the energy give good results up to  $I \sim 14$  in contrast to the  $I^2$  expansion previously described. The reason for the apparently more rapid convergence (at low spins) in  $\omega^2$  is not yet understood.

Of course, the recently observed transitions corresponding to decreasing  $\Delta E$  with increasing  $I$  imply, according to Eq. (5), that  $\omega$  first increases and then decreases (and finally increases again) with increasing  $I$ , making all quantities double- or triple-valued functions of  $\omega$  and thus implying a limited radius of convergence for any expansion in powers of  $\omega^2$ . As can be seen from Eq. (5), this backbending in  $\omega$  corresponds to the region of decreasing slope near the top of the ground-state band as shown in Fig. 2.

#### A. The $\mathcal{I}$ vs $\omega^2$ Plot

Because of the success of the VMI model and since the angular velocity  $\omega$  and moment of inertia  $\mathcal{I}$  are

easy to visualize, it has become customary to plot the  $\Delta E$  data in the form  $\mathcal{g}$  vs  $\omega^2$ . In the two-parameter Harris or VMI model, this plot would be a straight line.

Since the data consist of  $\Delta E_{I,I-2}$  for discrete even  $I$  values only, there is a minor ambiguity as to how the plot should be made. In order that each transition should (by itself) generate a point on the plot, and in order to give the expected result in the pure rotor limit, Eq. (2),  $\mathcal{g}$  is taken to be

$$2\mathcal{g}/\hbar^2 = (4I-2)/\Delta E_{I,(I-2)}. \quad (13)$$

The ambiguity arises in obtaining  $\omega$  from Eq. (5). The simplest method would be to use

$$(\hbar\omega)_{\text{simple}}^2 = [\Delta E_{I,(I-2)}/2]^2. \quad (14a)$$

The Brookhaven group "improves" the denominator by using

$$(\hbar\omega)_B^2 = \left\{ \frac{\Delta E_{I,(I-2)}}{[I(I+1)]^{1/2} - [(I-1)(I-2)]^{1/2}} \right\}^2. \quad (14b)$$

The Stockholm group further "improves" the denominator to allow for curvature by the use of

$$\begin{aligned} \Delta[I(I+1)]^{1/2} &= \{d[I(I+1)]^{1/2}/dI(I+1)\} \Delta I(I+1) \\ &= (2I-1)/(I^2-I+1)^{1/2}, \end{aligned} \quad (15)$$

and thus plots

$$(\hbar\omega)_s^2 = [\Delta E_{I,(I-2)}/(2I-1)]^2 [I^2-I+1]. \quad (14c)$$

All these forms are similar numerically for  $I$  values above  $I \sim 6$ , but there are significant differences for the lowest point or two, particularly if  $\mathcal{g}_0$  of Eq. (10) is small. In particular, the Brookhaven  $\mathcal{g}$  vs  $\omega^2$  plot using Eq. (14b) gives more nearly a straight-line behavior at small  $I$  for actual data while Eqs. (14a) and (14c) curve down as shown on Fig. 5. The data do fit VMI well at low spin so this down curving must be an artificial consequence of the method of plotting the data with Eqs. (14a) and (14c).

The data should most reasonably be plotted in such a way that a perfect two-parameter VMI nucleus will produce a straight line. By requiring that each data point produce one  $\mathcal{g}$  vs  $\omega^2$  point, this can be achieved in two limiting cases: (a) when  $C$  of Eq. (10) vanishes, and (b) when  $\mathcal{g}_0$  of Eq. (10) vanishes. Case (a) is the perfect rotor, and although case (b) may seem strange it is known that VMI fits some transition nuclei very well even with negative (Mariscotti, 1970; Scharff-Goldhaber and Goldhaber, 1970) values for the parameter  $\mathcal{g}_0$ .

The straight (horizontal) line for case (a) is assured by the use of Eq. (13). For case (b) we have

$$\mathcal{g} = a\omega^2, \quad (16)$$

where  $a$  is a constant. This yields the peculiar energy

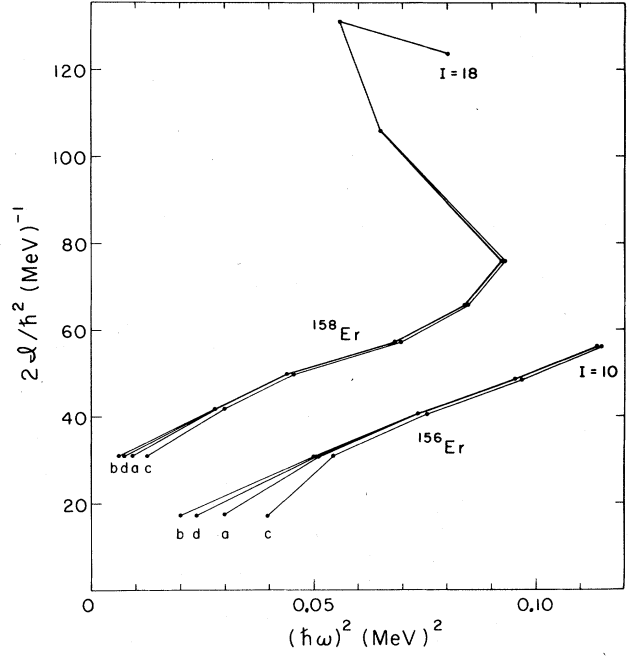


FIG. 5.  $\mathcal{g}$  vs  $\omega^2$  curves for  $^{156}\text{Er}$  and  $^{158}\text{Er}$ . The four curves a, b, c, and d correspond to different definitions of  $(\hbar\omega)^2$  in terms of the data as defined by the "simple" formula Eq. (14a), the "Brookhaven" formula Eq. (14b), the "Stockholm" formula Eq. (14c), and the VMI formula Eq. (14d). In each case  $\mathcal{g}$  is given by Eq. (13). The lowest dot is the  $I=2$  to 0 transition; next the 4 to 2 etc.

form

$$E_I = (3/4a^{1/3})[I(I+1)]^{2/3}, \quad (17)$$

as can be seen at once by checking that  $\omega = dE/d[I(I+1)]^{1/2}$  and  $[I(I+1)]^{1/2} = \omega\mathcal{g}$ . Then calculate  $\omega$  as

$$\hbar\omega = \Delta E_{I,(I-2)}/f(I), \quad (18)$$

where  $f(I)$  is so defined that if  $\Delta E$  is computed from Eq. (17) and  $\mathcal{g}$  from Eq. (13) a perfect straight line  $\mathcal{g}$  vs  $\omega^2$  plot results with the correct large  $I$  limit  $f(\infty) = 2$ . The resulting form is

$$(\hbar\omega)_{\text{VMI}}^2 = \frac{[\Delta E_{I,(I-2)}]^2(2I-1)}{(\frac{3}{2})^3 \{ [I(I+1)]^{2/3} - [(I-1)(I-2)]^{2/3} \}^3}. \quad (14d)$$

Numerically the coefficients in Eq. (14d) are much closer to those of the Brookhaven form [Eq. (14b)] than to either the simple form [Eq. (14a)] or the Stockholm form [Eq. (14c)]. All the forms converge at the higher spins.

The use of Eqs. (13) and (14d) will produce a straight line plot for a perfect two-parameter VMI nucleus for  $\mathcal{g}_0=0$  or for  $C=0$  of Eq. (10), and do a reasonable job for intermediate cases as well. If  $C$  of Eq. (10) is small, but not zero (more precisely if  $C/\mathcal{g}_0^3$

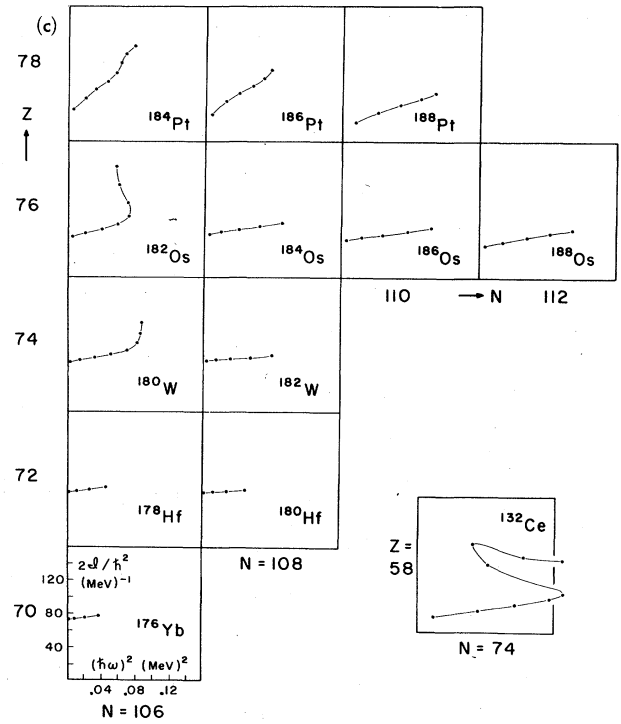
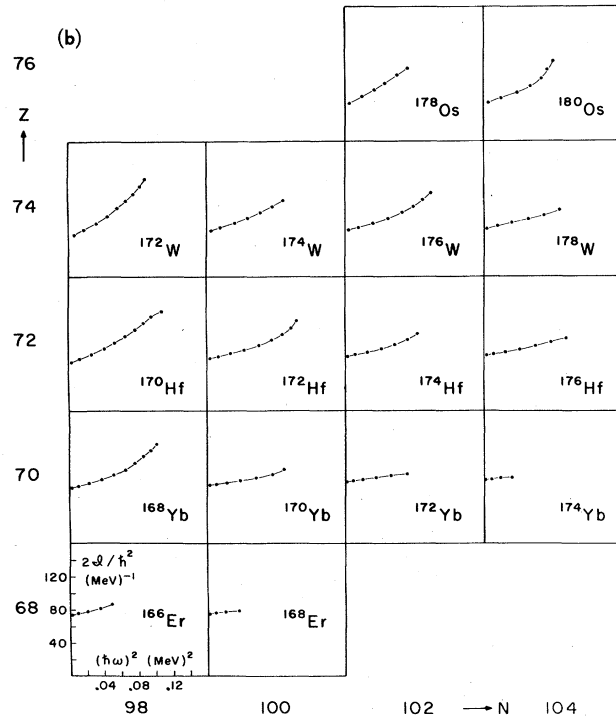
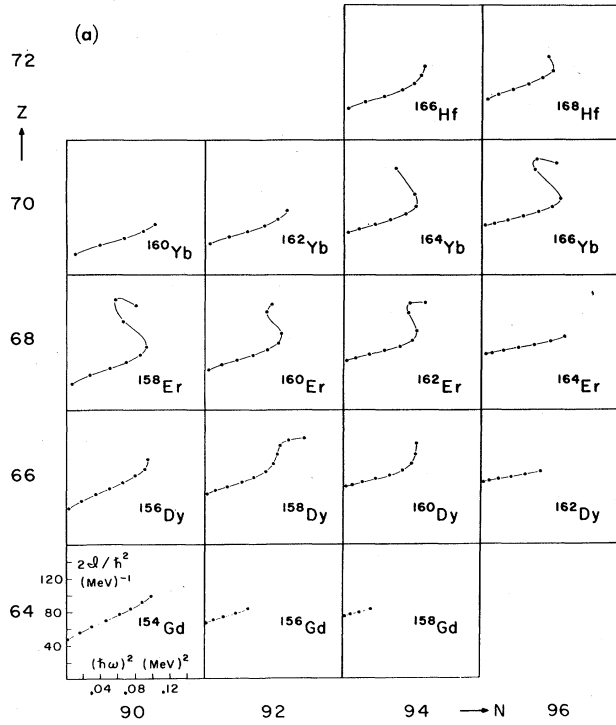


FIG. 6. (a), (b), (c).  $\Delta$  vs  $\omega^2$  curves of the rare-earth region. The data are plotted with the use of Eqs. (13) and (14d).

is much less than one), then it can be shown that the Stockholm form [Eq. (14c)] should give the best fit to VMI, but in such cases there are relatively small differences between the different formulas. By comparing these formulas with the actual transition energy data over the entire rare-earth region, it is found that in about 80% of all cases the Brookhaven form (14b) or the new form (14d) are superior to the form (14c) in producing a straight line fit to the lowest three transition energies.

### B. The Data

Figure 6 shows plots of  $\mathcal{J}$  vs  $\omega^2$  for the rare-earth region taken from a compilation prepared by the Stockholm collaboration (Saethre, 1972). It is seen that sharp increases in  $\mathcal{J}$  are observed in a number of nuclei from Dy to Os ( $66 \leq Z \leq 76$ ) with neutron numbers from the lower edge to almost the end of the region ( $90 \leq N \leq 106$ ). The break occurs at about  $I=14-16$ . Backbending (S-shaped curves) occur for some Er, Yb, Hf, and Os isotopes. Whether or not the same behavior occurs for the lighter deformed  ${}_{64}\text{Gd}$  and  ${}_{62}\text{Sm}$  isotopes is not known since the high spin states,  $I > 14$ , have not been observed. However, a sharp backbending has been observed in  ${}_{58}^{132}\text{Ce}_{74}$  (Taras *et al.*, 1972). Concerning the heavier W, Os, and Pt deformed nuclei, the situation is not clear. The sudden increase in moment of inertia thus seems to be a rather general phenomenon in the rare-earth region, with the detailed picture of the  $N$  and  $Z$  dependence of the degree of singularity beginning to emerge. While there are sudden jumps for all  $Z$  values, it seems that the curves for  $N \approx 98, 100$  are smoother than those for larger or smaller  $N$  values. Further experimental work is still needed.

For one of the strongly backbending nuclei,  ${}^{158}\text{Er}$ , the recoil distance "plunger" technique has been used to determine the lifetimes and thus the  $B(E2)$  values for each transition up to the top of the band at spin 18 (Ward *et al.*, 1973). The results are shown in Table I. All the transitions are seen to be of the order of enhanced rotational collective rates, but the  $I=14-12$  transition in the backbending part of the curve has a

rate which is clearly reduced from the average of the neighboring rates by about 20 to 40%. Some such reduction is expected where the nucleus is changing its structure as will be discussed in Secs. IVG2 and V.

For the construction of models of the process, it would also be valuable to have more information about the transitions preceding the observed lines of the ground-state band. In addition to the short times already known (Diamond *et al.*, 1969), the Brookhaven group (Sunyar *et al.*, 1972) has made a beginning by estimating the average number of  $\gamma$ 's from a study of the background.

### III. THEORETICAL DESCRIPTIONS

The theoretical description of this phenomena has been made on three different levels. First there have been phenomenological semiclassical models in which a few parameters are introduced with little attempt at connection with a microscopic theory. Such calculations will be discussed below. Then there have been microscopic calculations which will be discussed at length in the sections following the presentation of the cranking model. Finally, there are mixed calculations in which a few of the nucleons are treated explicitly while the rest form a rotating core with which they interact. Such calculations will be discussed at the end of the paper.

The success of the VMI model (before the recent experiments) prompted picturesque descriptions of these results. Trainor and Gupta (1971) ascribe the increasing moment of inertia to a geometrical picture of a deformed nucleus in which an inscribed sphere of nuclear matter is not rotating at all, and the outer deformed shell is rotating rigidly. The separation of the nucleus into nonrotating and rotating nucleons with a sharp geometrical slippage surface seems absurd, but the microscopic models also have some slippage due to the superconducting (superfluid) nature of the nuclear matter. Other modifications of the VMI model have also been treated (Satpathy and Satpathy, 1971; Gupta, 1971).

The sudden rise in  $\mathcal{J}$  and the backbending  $\omega^2$ , however, require a more significant change in the VMI parameterization. The addition of another term in the Harris  $\omega^2$  expansion to make a three-parameter VMI fit (Saethre *et al.*, 1972) can only help a little, below this singularity. Wahlborn and Gupta (1972) obtain good fits to low and high spin data with a parameterized formula specifically designed to resemble the VMI at low spin, but capable of reproducing the S-shaped  $\mathcal{J}$  vs  $\omega^2$  plot. Molinari and Regge (1972) consider algebraic forms related to possible singularities in the complex angular momentum plane.

Thieberger notes that the sudden rise in  $\mathcal{J}$  can be described within the VMI model in terms of an intrinsic energy function [see Eq. (9)]  $V(\mathcal{J})$  which rises some-

TABLE I.  $B(E2)$  values for  ${}^{158}\text{Er}$  from Ward *et al.* (1973).

Transition	$B(E2)/ROT$
2-0	1
4-2	$1.10 \pm 0.05$
6-4	$1.31 \pm 0.27$
8-6	$1.17 \pm 0.40$
10-8	$1.20 \pm 0.56$
12-10	$\lesssim 1$
14-12	$0.80 \pm 0.19$
16-14	$1.40 \pm 0.35$
18-16	$> 0.6$

what less rapidly than quadratically in  $\mathcal{J} - \mathcal{J}_0$ . He points out that  $V(\mathcal{J})$  can be obtained directly from the experimental  $\mathcal{J}$  vs  $\omega^2$  data by integrating Eq. (8) to get (Thieberger, 1972b)

$$V(\mathcal{J}) = \int_{\mathcal{J}_0}^{\mathcal{J}} \frac{1}{4} (\hbar\omega)^2 d \left( \frac{2\mathcal{J}}{\hbar^2} \right). \quad (19)$$

Draper (1972) fits the backbending data (but not the full  $S$  curve) by a specific choice for the replacement of Eq. (9). He replaces the quadratic form  $[(\mathcal{J} - \mathcal{J}_0)/\mathcal{J}_0]^2$  with the more slowly varying form

$$V(\mathcal{J}) = V_0 + \text{Const} \times [\ln(\mathcal{J}/\mathcal{J}_0)]^2. \quad (20)$$

As can be seen from the expansion of  $\ln$  about argument unity, it is clear that this will approximate the usual two-parameter VMI model until  $\mathcal{J}/\mathcal{J}_0$  is significantly greater than unity, and then produce the more rapidly rising moment of inertia.

The phenomenological models just described do not really specify the physical change under rotation. Does the nucleus stretch, become unpaired, or change its shape or interparticle correlations in some other way as it rotates? To answer these questions, the model must be described in terms of the particles to be correlated and thus must be a microscopic theory.

#### IV. THE CRANKING MODEL

Nearly all of the fully microscopic theories of nuclear rotation are based on or related to some version of the cranking model of Inglis (1954).<sup>1</sup> A readable derivation is given by Villars (1957). In view of its importance it is appropriate to give a derivation here.

An elementary presentation follows in which the derivation of the "cranking model" moment of inertia is compared step by step with the analogous "pushing model" formula for the mass. The basic assumption of the simplest form of the cranking model (pushing model) is that the nuclear many-body system in its rotation (translation) can be described in terms of independent noninteracting particles contained in an external potential well which is rotating (translating). This assumption has been modified and tested, as will be discussed later, but on this simple basis the problem is to calculate the energy of the system as a function of the angular velocity  $\omega$  (linear velocity  $v$ ) with which the potential is moving. The energy should increase with  $\omega(v)$  quadratically, at least at small angular velocities, and the coefficient in  $E = \frac{1}{2} \mathcal{J} \omega^2$  ( $E = \frac{1}{2} M v^2$ ) is identified as the moment of inertia  $\mathcal{J}$  (mass  $M$ ).

<sup>1</sup> Although Inglis' formula for the moment of inertia and much of his discussion in the 1954 paper was correct and most illuminating, his derivation of the cranking formula was wrong, but corrected by the author in the appendix of a later paper (Inglis, 1956). The error is also pointed out and corrected by Valatin (1956).

Thus the time-dependent Schrödinger equation

$$H(t)\psi = i\hbar\dot{\psi} \quad (21)$$

must be solved, where the Hamiltonian

$$H(t) = p^2/2m + V(t) \quad (22)$$

is time-dependent since the potential of fixed shape is moving in space with a constant angular (linear) velocity. For the pushing case, if at  $t=0$  the potential is  $V(0) = g(x, y, z)$ , and the potential is translating in the  $+z$  direction with velocity  $v$ , the time-dependent form is

$$V(t) = g(x, y, z - vt). \quad (23p)$$

For the cranking case, for rotation about the  $z$  axis, the time-dependent form is

$$V(t) = h(r, \theta, \phi - \omega t), \quad (23c)$$

where the  $t=0$  potential shape must have a dependence on  $\phi$ , that is, it must be a deformed nonspherical potential.

Because of the very simple time dependence of Eqs. (23), a simple but time dependent unitary transformation can be found to eliminate the time dependence of the transformed Hamiltonian. It is

$$U = \exp(ivt p_z / \hbar) \quad (24p)$$

$$U = \exp(i\omega t L_z / \hbar). \quad (24c)$$

Then rewrite Eq. (21) as

$$UH(t)U^{-1}U\psi = i\hbar U\dot{\psi}. \quad (25)$$

Since Eq. (24) is a rotation (translation) operator

$$Ug(z)U^{-1} = g(z + vt), \quad (26p)$$

$$Uh(\phi)U^{-1} = h(\phi + \omega t), \quad (26c)$$

the original time-dependent Schrödinger equation becomes

$$H(0)U\psi = i\hbar U\dot{\psi}, \quad (27)$$

where  $H(0)$  is time-independent and equal to  $H(t)$  at  $t=0$ . Then define

$$\psi_T = U\psi \quad (28)$$

so that Eq. (27) becomes

$$H(0)\psi_T = i\hbar\dot{\psi}_T - i\hbar\dot{U}\psi. \quad (29)$$

The partial differentiation of  $U$  gives, after rearrangement,

$$[H(0) - vp_z]\psi_T = i\hbar\dot{\psi}_T \quad (30p)$$

$$[H(0) - \omega L_z]\psi_T = i\hbar\dot{\psi}_T. \quad (30c)$$

Equation (30) is a time-dependent Schrödinger equation, but with an explicitly time-independent effective Hamiltonian. Thus it can be solved as an eigenvalue problem in the standard way. The Inglis formula results from a perturbation treatment based on eigenfunctions of  $H(0)$  with  $\omega(v)$  assumed to be very small.



that is

$$H(0) |i\rangle = E_i^{(0)} |i\rangle, \quad (31)$$

and for the ground state

$$\psi_T \cong |0\rangle + v \sum_i [\langle i | p_z | 0\rangle / (E_i^{(0)} - E_0^{(0)})] |i\rangle, \quad (32p)$$

$$\psi_T \cong |0\rangle + \omega \sum_i [\langle i | L_z | 0\rangle / (E_i^{(0)} - E_0^{(0)})] |i\rangle, \quad (32c)$$

$$E_T \cong E_0^{(0)} - v^2 \sum_i |\langle i | p_z | 0\rangle|^2 / (E_i^{(0)} - E_0^{(0)}), \quad (33p)$$

$$E_T \cong E_0^{(0)} - \omega^2 \sum_i |\langle i | L_z | 0\rangle|^2 / (E_i^{(0)} - E_0^{(0)}); \quad (33c)$$

the  $|0\rangle$  expectation for  $L_z(p_z)$  vanishes and the first correction to the energy comes in second order.

The quantity  $E_T$  of Eq. (33) is the ground-state energy of the effective Hamiltonian on the left side of Eq. (30). But, the energy to be associated with the rotational (translational) inertia is the energy associated with the original time-dependent Eq. (21), namely,

$$E = \langle \psi | H(t) | \psi \rangle = \langle \psi_T | H(0) | \psi_T \rangle. \quad (34)$$

This can be written

$$E = E_T + v \langle \psi_T | p_z | \psi_T \rangle \quad (35p)$$

$$E = E_T + \omega \langle \psi_T | L_z | \psi_T \rangle. \quad (35c)$$

If Eq. (32) is used to evaluate  $\psi_T$  in Eq. (35) the result is

$$E = E_0^{(0)} + v^2 \sum_i |\langle i | p_z | 0\rangle|^2 / (E_i^{(0)} - E_0^{(0)}) = E_0^{(0)} + \frac{1}{2} M v^2, \quad (36p)$$

$$E = E_0^{(0)} + \omega^2 \sum_i |\langle i | L_z | 0\rangle|^2 / (E_i^{(0)} - E_0^{(0)}) = E_0^{(0)} + \frac{1}{2} \mathcal{I} \omega^2, \quad (36c)$$

giving the cranking formula for the moment of inertia

$$\mathcal{I} = 2 \sum_i |\langle i | L_z | 0\rangle|^2 / (E_i^{(0)} - E_0^{(0)}). \quad (37c)$$

With the inclusion of spin,  $L_z$  should be replaced by  $J_z$ , the total angular momentum operator.

### A. The Pushing Model Result

The formula [Eq. (37c)] must be treated with great care as will be seen, so it is fortunate to have the parallel discussion of the pushing model for which the exact result is known as a test case. In the pushing model, if  $H(0)$  is simply the sum of particle kinetic energies and a potential energy depending only on coordinates (no velocity dependence), then it is not necessary to use perturbation theory as in Eqs. (32) and (33), and an exact solution of Eq. (30p) is easily obtained. This exact result (to all orders in  $v$ ) is identical with the perturbation result of Eq. (36p); namely

$$M = 2 \sum_i |\langle i | p_z | 0\rangle|^2 / (E_i^{(0)} - E_0^{(0)}). \quad (37p)$$

It is encouraging that Eq. (37p) is in fact an exact and correct result as can be seen from the commutator relation

$$[p_z^2, Z] = -2i\hbar p_z \quad (38)$$

so that

$$[H(0), Z] = -i(\hbar/m) p_z \quad (39)$$

for each particle.

Then Eq. (37p) becomes, for the many-body case represented by the particle number index  $\alpha$  and  $\beta$ ,

$$\begin{aligned} M &= \sum_{\alpha\beta} 2 \sum_i \langle 0 | p_{z\alpha} | i \rangle \langle i | p_{z\beta} | 0 \rangle / (E_i^{(0)} - E_0^{(0)}) \\ &= \sum_{\alpha\beta} (2im/\hbar) \\ &\times \sum_i \langle 0 | p_{z\alpha} | i \rangle \langle i | [H(0), Z_\beta] | 0 \rangle / (E_i^{(0)} - E_0^{(0)}) \\ &= \sum_{\alpha\beta} (im/\hbar) [\langle 0 | p_{z\alpha} Z_\beta | 0 \rangle - \langle 0 | Z_\beta p_{z\alpha} | 0 \rangle] \\ &= \sum_{\alpha\beta} m \delta_{\alpha\beta} = \sum_{\alpha} m. \end{aligned} \quad (40)$$

There is no analogous result for the cranking case both because (37c) is a perturbation result and not exact in that case, and because there is no operator whose commutator with  $H(0)$  is  $L_z$  as there is in the pushing case of Eq. (39).

Since the rotational result [Eq. (40)] depends only on the commutation relation Eq. (39), it is clear that it is correct also in the case of the particles interacting with each other as well as with the moving potential; that is,  $H(0)$  need not be an independent particle Hamiltonian. In contrast, the particle-particle interactions play a vital role in the cranking case.

Observe that in the derivation as presented here, the effective Hamiltonian on the left side of Eq. (30) does *not* represent the Hamiltonian as seen from a moving coordinate system. The time-dependent unitary transformation  $U$  of Eq. (24) is a transformation to moving coordinates, but the corresponding transformation to new momenta was not made. Indeed, had the full Galilean transformation to a moving coordinate system been performed, including transformation of the momenta, the effective Hamiltonian for the pushing case would have been  $H(t)$  at  $t=0$  without the extra term  $-vp_z$ , as there are no new inertial effective forces produced by a uniform translation.

However, there are effective inertial forces in the case of rotation, namely Coriolis and centrifugal forces. If a complete transformation to rotating coordinates is made including transformation of the momenta, the Hamiltonian as seen in the rotating system and in terms of the new coordinates and momenta is

$$H_\omega = H(0) - \omega L_z, \quad (41)$$

the same form as Eq. (30c). In this expression the term  $-\omega L_z$  generates both the Coriolis and centrifugal force of the rotating coordinate system. This is the

interpretation of the term  $-\omega L_z$  given by Inglis (1956), Valatin (1956), and Brown (1964).

Equation (41) can be directly derived from the well-known expressions for the Coriolis and centrifugal forces (Corben and Stehle, 1950):

$$F_{\text{Coriolis}} = -2m\boldsymbol{\omega} \times \dot{\mathbf{r}} \quad (42)$$

$$F_{\text{Centrifugal}} = -m\boldsymbol{\omega} \times (\boldsymbol{\omega} \times \mathbf{r}). \quad (43)$$

For constant  $\boldsymbol{\omega}$  in the  $z$  direction the centrifugal force is described by a potential

$$V_c = -\frac{1}{2}m\omega^2\rho^2, \quad (44)$$

where  $\rho$  is the cylindrical coordinate. The Coriolis force is equivalent to the presence of a uniform magnetic field in the  $z$  direction with  $B=2m\omega$  which can be described with an appropriate vector potential  $\mathbf{A}=\frac{1}{2}\mathbf{B} \times \mathbf{r}$  so that

$$\mathbf{A} = m\boldsymbol{\omega} \times \mathbf{r}. \quad (45)$$

Then the kinetic plus inertial forces operator becomes

$$T = (2m)^{-1}(\mathbf{p} - m\boldsymbol{\omega} \times \mathbf{r})^2 + V_c. \quad (46)$$

The  $\omega^2$  terms cancel and the result is

$$T = (\mathbf{p}^2/2m) - \boldsymbol{\omega} \cdot \mathbf{L}, \quad (47)$$

which gives Eq. (41). The ground-state eigenvalue of Eq. (41) is of course not the lab energy required in Eq. (35) and instead the wave functions resulting from Eq. (41) must be transformed back to the lab system and the energy calculated in that system. The result is the same as before, namely Eq. (37c). Although the rotating coordinate system interpretation of Eq. (41) can give helpful physical insight for its eigenfunctions, the transformation back to the lab to obtain the energy Eq. (36c) is not so obvious.

## B. Interpretation of the Cranking Formula

A valid use of the cranking formula must answer the fundamental question of just what is the rotating potential of Eq. (22), but first the early discussions will be outlined as they show some of the subtlety of the evaluation of Eq. (37c).

The cranking model was first used by Wick (1948) to calculate the electronic flow in a rotating molecule. In this case the slowly rotating potential in which the electrons move is generated in large measure by the heavy nuclei and the cranking approximation should be good. The result is that the electrons do not rigidly follow the rotation of the nuclei. In fact they slip somewhat, thus producing a smaller current in the lab than that implied by a rigid rotation. In particular, Wick showed that for a single electron in its ground-state wave function (with no nodes) the flow is irrotational independent of the form of the potential.

Inglis (1954) found furthermore that the moment of inertia calculated according to Eq. (37c) gives the

irrotational flow value for a many-body system consisting of nucleons moving in an anisotropic (deformed) harmonic oscillator potential

$$H(0) = \mathbf{p}^2/2m + \frac{1}{2}(\omega_x^2 x^2 + \omega_y^2 y^2 + \omega_z^2 z^2), \quad (48)$$

with  $\omega_x \neq \omega_y \neq \omega_z$ , and quantum numbers of occupied states corresponding to full spherical shells, i.e., all states occupied to principal quantum number  $N$ ,

$$n_x = n_y = n_z = N/3. \quad (49)$$

The  $n_x, n_y, n_z$  are the usual one-dimensional harmonic oscillator quantum number for the  $x, y$ , and  $z$  degrees of freedom. The resulting irrotational moment of inertia is proportional to  $\beta^2$  or to  $(\omega_y - \omega_z)^2$ , the square of the deformation parameter (cranking about the  $x$  axis as is conventional).

To be precise we have

$$\mathcal{I}_{\text{irrot}} = \mathcal{I}_{\text{rigid}}\epsilon^2, \quad (50)$$

where

$$\epsilon = (R_{\text{major}} - R_{\text{minor}})/R_0 \cong 0.95\beta. \quad (51)$$

Since the experimental moments of inertia are four to five times the irrotational value there was some effort to *increase* the theoretical value by considering residual interactions, departures from the oscillator shape, etc., but Bohr and Mottelson (1955), who were the first to recognize the vital importance of treating the nuclear shape self-consistently, showed that the simple cranking model in fact yields the rigid value for the moment of inertia, which is two to three times bigger than the experimental values. These results were discussed and amplified by Inglis (1956) and by Moszkowski (1956).

For a general configuration of occupied states in the deformed harmonic oscillator potential, the cranking model moment of inertia Eq. (37c) is easily computed to be (Bohr and Mottelson, 1955)

$$\mathcal{I} = (\hbar/2\omega_y\omega_z) \left\{ \left[ \frac{(\omega_y - \omega_z)^2}{(\omega_y + \omega_z)} \right] \sum (n_y + n_z + 1) + \left[ \frac{(\omega_y + \omega_z)^2}{(\omega_y - \omega_z)} \right] \sum (n_x - n_y) \right\}, \quad (52)$$

where the sums are over the occupied state quantum numbers. The first term gives the Inglis irrotational result of Eqs. (49)–(50), but for the closed-shell configuration of Eq. (49) the self-consistent nuclear shape (solution of the Hartree-Fock equations) is spherical and there is no deformed potential to crank.

For any other configuration, with one or more particles beyond the “spherical” closed shells represented by Eq. (49), the equilibrium (self-consistent) shape is deformed. For small numbers of particles outside of closed shells the deformation is proportional to that number. Specifically, Mottelson showed that the requirement that the particle density deformation equal the deformation of the potential of Eq. (48) leads to the result that the total nuclear deformation is produced half by the extra particles (outside of closed

shells) and half by the core of closed-shell particles (Mottelson, 1962).

Thus, for one or two particles outside closed shells, while  $\sum (n_z - n_y)$  is small, the deformation and thus  $(\omega_y - \omega_z)$  is also very small so that the second term of Eq. (52) is large and more important than the first term. Careful calculation shows that for any number of particles beyond closed shells the second term of Eq. (52) is just large enough, if the  $\omega$ 's are calculated for a self-consistent deformation, so that the resulting calculated moment of inertia is exactly the rigid value,

$$I_{\text{rigid}} = \sum m_i (y_i^2 + z_i^2), \quad (53)$$

where the sum is over *all* the particles including those of the "spherical closed-shell" quantum numbers.

This result, which is exact for any number of extra core particles for the harmonic oscillator potential, is expected to hold for independent particles in any potential in the  $n \rightarrow \infty$  limit (Bohr and Mottelson, 1955) and to be approximately valid for finite  $n$ . The crucial importance of self-consistency is seen from the fact that Eq. (52) can be made to yield any value from irrotational to even larger than the rigid moment of inertia if the deformation and configuration may be chosen independently. The pushing model (for linear motion) does not involve the type of self-consistency just discussed; its moving well may be either self-consistent or externally imposed so that a comparison of the pushing and cranking models cannot help to clarify this particular point.

### C. The Effect of Residual Interactions

Since the rigid value is two to three times larger than the experimental moments of inertia, the problem was thus to find some effects to *lower* the theoretical value. Bohr and Mottelson (1955) correctly indicated that residual two-body interactions not included in the one-body Hartree-Fock field would lower the moment, and that correlations of the pairing type would be the most important.

Calculating the change in moment of inertia due to two-body interactions is not simple, as shown by Amado and Brueckner (1959). In this paper it is shown that for particles in plane wave states with periodic boundary conditions in a cubic box, the cranking formula Eq. (37c) gives the rigid moment of inertia in the  $n \rightarrow \infty$  limit. The importance of self-consistency is not mentioned but is, of course, automatically satisfied for such a "nuclear matter" type wave function.

It is then demonstrated that the addition of any two-body interaction, including one which would alter the level density, has no effect on the cranking moment of inertia to first order in the added interaction. The effect of the changed denominators in Eq. (37c) is cancelled by a compensating effect in the  $L_z$  matrix elements to first order. Rockmore (1959) then showed

that the same result, namely unchanged rigid moment of inertia, holds to all orders of the random phase approximation (RPA) treatment of the particle-hole part of the added two-body interaction.

### D. Moment of Inertia with Pairing

This is not the case for pairing correlations (Rockmore, 1960). In fact, Belyaev (1959) showed explicitly that residual interactions of the pairing type (particle-particle scattering to hole-hole states) denoted by BCS (Bardeen, Cooper, and Schrieffer, 1957; Bogoliubov, 1958, 1958a, 1958b; Valatin, 1958) do indeed lower the moment of inertia from the rigid value. There are two effects both working in the same direction to lower the value of Eq. (37c). First, the energy denominator  $E_i^{(0)} - E_0^{(0)}$ , which is simply the particle-hole excitation energy  $\epsilon_p - \epsilon_h$ , becomes for the paired system

$$E_i^{(0)} - E_0^{(0)} = E_p + E_h, \quad (54)$$

where

$$E_n = [(\epsilon_n - \lambda)^2 + \Delta^2]^{1/2} \quad (55)$$

is the quasiparticle energy, thus implying an increased energy denominator if the gap parameter  $\Delta$  is non-vanishing. The second effect is a reduction of the  $L_z$  matrix element by the factor  $(U_p V_h - U_h V_p)$  which appears squared in the numerator of Eq. (37c). The quantities  $\lambda$  and  $V$  are the Fermi energy and occupation probability parameters of pairing theory (Bés and Sorensen, 1969) and  $U^2 = 1 - V^2$ .

The resulting moment of inertia formula

$$I = 2 \sum_{\nu\nu'} [ | (J_z)_{\nu\nu'} |^2 / (E_\nu + E_{\nu'}) ] (U_\nu V_{\nu'} - V_\nu U_{\nu'})^2 \quad (56)$$

was evaluated for realistic nuclear parameters by Griffin and Rich (1960) and by Nilsson and Prior (1961). In these calculations, the all important self-consistency is put in by use of the Nilsson model (1955) (see also Mottelson and Nilsson, 1959), single-particle energies. This is a modified deformed harmonic oscillator model which includes a deformation dependence of the average oscillator parameter to simulate nuclear volume conservation under deformation. With parameters chosen primarily to fit odd mass nuclear levels, the model gives self-consistent deformations for even deformed nuclei in reasonable agreement with observed  $B(E2)$  values. The self-consistency involves a minimization of the sum of occupied single-particle energies as a function of deformation, which is thought to be equivalent to a Hartree (Fock) self-consistency for the special case of an harmonic self-consistent potential form. The calculation of the moment of inertia is not precisely self-consistent, however, since the deformation  $\beta$  used is taken to fit the experimental  $B(E2)$  value for each nucleus. Likewise the pairing parameters are not derived from a two-body force, but chosen to fit experimental data particularly concerning odd-even mass differences.

The result is a remarkable agreement with the experimental values. The fine structure of variation from nucleus to nucleus is well reproduced for both the rare earth and the actinide nuclei, but the "best" choice of parameter values leads to slightly too small values for the theoretical moments of inertia. That is, the pairing produces a little too much lowering from the rigid moment.

This lowering of the moment of inertia corresponds to a superfluid slippage of some fraction of the nucleus as the nucleus rotates (Migdal, 1959, 1959a). Since the neutrons and protons are paired separately for heavy nuclei the fractional slippage may not be the same for each, so that the gyromagnetic ratio  $g_R$ , which is a result of the proton current, might differ from  $Z/A$ , the value obtained assuming spins to be paired and protons and neutrons moving together. Experimentally,  $g_R$  for  $2+$  rotational excited states is somewhat less than  $Z/A$ , a result in general good agreement (Nilsson, 1961; Migdal, 1959) with the observation that the pairing in deformed nuclei is somewhat stronger for protons than for neutrons ( $\Delta_p > \Delta_n$ ) as observed in the experimental odd-even mass differences.

The success of these calculations which finally produced semiquantitatively correct moments between the far too small irrotational value and the too large rigid value is convincing evidence that our picture of rotational nuclei as deformed, superfluid many-body systems is qualitatively correct.

### E. The Mottelson-Valatin Effect (Basic Idea)

The new data of interest in this article concern the change in the moment of inertia as a function of angular momentum or angular velocity rather than its value at  $\omega=0$  which has been the topic of discussion in this section up to this point. The self-consistency problem for the variation of the moment of inertia is clearly much more difficult than that for the  $\omega=0$  case. While in the latter case it was possible to almost completely avoid the self-consistency problem by the use of other experimental information concerning deformations and the strength of pairing, little or no such direct data concerning the change in deformation and pairing exists for high angular momentum states, and in fact it should be the aim of the calculation to predict such changes as well as the changes in the moment of inertia. Even for small changes in the ground-state parameters (and the measured high spin states must involve large changes in some parameters since the moment of inertia changes by a factor of two and more in some cases) a simple higher order perturbation treatment would not be valid, and at the very least an appropriate self-consistent perturbation theory must be applied.

At this point, Mottelson and Valatin (1960) made their observation that at a sufficiently high angular

velocity the nuclear pairing correlations should be reduced to zero, in analogy to the destruction of superconductivity in the presence of a sufficiently strong magnetic field, the Meissner effect. The analogy with superconductivity in a magnetic field arises from the fact that the Coriolis force as seen in the rotating coordinate system, Eq. (42), is equivalent to the imposition of a magnetic field as noted in Eq. (45).

The physical origin of the Coriolis antipairing effect is as follows. For a nucleus described as a nonrotating deformed potential, the single-particle orbits occur as degenerate time reverse pairs. The attractive pairing force has large matrix elements for pairs of nucleons occupying (or scattering between) such time reverse paired orbitals. When the nucleus or potential is rotating, the individual nucleons feel (in a coordinate system rotating with the potential) not only the deformed potential, but also centrifugal and Coriolis forces. The Coriolis forces break the time reverse degeneracy, lowering those states with angular momentum pointing toward the rotation direction relative to those pointing away. This tilting of the single-particle orbits tends to break the pairs favored by the pairing force and to align the individual particle angular momenta in the direction of rotation. For sufficiently rapid rotation, the pairing correlations should disappear.

At the time of this prediction of the Mottelson-Valatin Coriolis antipairing CAP effect, there was no data to sufficiently high spin to test the idea. By considering the competition between the binding energy gain due to the pairing correlations in the rotating coordinate system, and the loss of binding (or increase in rotational energy) owing to the reduced moment of inertia caused by pairing, Mottelson and Valatin were able to estimate the spin value  $I_c$  above which the self-consistent pairing should vanish. At higher spins they predicted a moment of inertia equal to the rigid value in accordance with the rather general cranking result in the absence of pairing correlations, and furthermore predicted a rather sudden change in the wave function at  $I \sim I_c$  from the correlated to uncorrelated form which would cause the ground-state band, as seen in multiple Coulomb excitation, effectively to terminate at  $I = I_c$ . Their estimate was  $I_c = 12$  for  $A = 180$  and  $I_c = 18$  for  $A = 238$ , in remarkably good agreement with the presently observed sudden increases in moments of inertia of a number of rare-earth nuclei beginning at about spin 14-16.

### F. Theory of Rotation

During this period there were a number of attempts to discuss nuclear rotation from first principles, without resorting to the cranking model. Peierls and Yoccoz (1957) (Yoccoz, 1957) performed an approximate variational calculation based on the Hill-Wheeler (1953) (Griffin and Wheeler, 1957) generator coordinate idea.

They minimize the Hamiltonian expectation for a linear combination of deformed axially symmetric independent particle wave functions  $\Phi_{\theta,\phi}(\mathbf{x})$ , the linear combination corresponding to different orientations of the direction  $\theta, \phi$  of the symmetry axis. The trial wave function is thus

$$\psi(\mathbf{x}) = \int d\theta d\phi \chi(\theta, \phi) \Phi_{\theta,\phi}(\mathbf{x}). \quad (57)$$

The variational condition

$$\delta E = \delta(\langle \psi | H | \psi \rangle / \langle \psi | \psi \rangle) = 0 \quad (58)$$

in this case is equivalent to deformed projected Hartree-Fock, and the weight function  $\chi$  is proportional to  $Y_{lm}(\theta, \phi)$ . For large deformations and thus small overlap between deformed wave functions corresponding to different orientations it is shown that the resulting energy is of the form

$$E_{lm} = E_0 + cl(l+1) \quad (59)$$

allowing a definition of the moment of inertia. The actual evaluations with nuclear forces were not done self-consistently, an impossibly difficult job at the time, but furthermore this formulation was known not to give the correct result for the pushing model, a very serious failing.

The method needed to find agreement between this sort of theory and the pushing model result, and at the same time to justify the Inglis cranking formula was given by Gross (1959).

Instead of taking for the trial wave function one corresponding to a linear combination of states with different orientations of the symmetry axis (different positions in the pushing case), thus projecting to a definite angular (linear) momentum, one takes a trial function corresponding to a linear combination of states with different angular (linear) velocities. The wave function can be forced to satisfy the condition that the expectation value of the angular (linear) momentum take on a fixed value. The wave function resulting from the variational condition Eq. (58) may in addition be projected to a definite angular (linear) momentum.

The result for the case of linear momentum is

$$E = E_0 + (P^2/2mA), \quad (60)$$

where  $P$  is the momentum expectation and  $A$  the number of particles. The correct mass is obtained whether or not the final projection to definite linear momentum is performed, although of course a lower  $E_0$  results from projection. The resulting wave function for the moving system is just  $\exp[(mv/\hbar) \sum x_\alpha]$  times the translation invariant function for  $P=0$ .

In the rotational case it is shown that

$$E = E_0 + (I^2/2\mathcal{J}), \quad (61)$$

where

$$\langle \psi | J_x | \psi \rangle = I, \quad (62)$$

the fixed angular momentum expectation value, and in the case of no projection to definite angular momentum the moment of inertia  $\mathcal{J}$  is given by the Inglis formula [Eq. (37c)].

The connection with Hartree-Fock theory is carefully worked out by Thouless (1960), Thouless and Valatin (1960, 1962), and Peierls and Thouless (1962). The problem is to determine what Slater determinant  $\phi$  will minimize the nuclear Hamiltonian  $H = \sum T_\alpha + \sum V_{\alpha\beta}$  with the constraint that  $\langle \phi | J_x | \phi \rangle = I$  is satisfied. The unconstrained solution  $|\phi_0\rangle$  must of course have a deformed shape, and will have  $\langle \phi_0 | J_x | \phi_0 \rangle = 0$ .

The method of Lagrange multipliers is used to enforce the constraint condition, so that

$$H' = H - \omega J_x \quad (63)$$

must be minimized where  $\omega$  is the Lagrange multiplier. Observe that the auxiliary Hamiltonian  $H'$  has the same form as that of Eq. (30c). For small  $\omega$  and thus small  $I$ , the second term of Eq. (63) may be treated in perturbation theory using  $|\phi_0\rangle$  and particle-hole excited states based on  $|\phi_0\rangle$  as basis states.  $|\phi\rangle$  is written as

$$|\phi\rangle = \prod_{i,n} (1 + C_{ni} a_n^\dagger a_i) |\phi_0\rangle, \quad (64)$$

where  $n, m$  are unoccupied and  $i, j$  occupied states of  $|\phi_0\rangle$  and  $C_{ni}$  the particle-hole admixture coefficients. The Hartree-Fock unperturbed single-particle and hole energies are  $\epsilon_n$  and  $\epsilon_i$ . The perturbation equations determining the admixture coefficients  $C_{ni}$  are not the usual ones of ordinary perturbation theory since the unperturbed variation giving  $|\phi_0\rangle$  is equivalent to the well known self-consistent problem. That is, the one-body Hartree-Fock Hamiltonian  $\sum h_\alpha$  giving the  $\epsilon_i, \epsilon_n$  as eigenvalues contains the one-body part of  $H$ , namely the kinetic energy  $\sum t_\alpha$ , but it also contains the self-consistent potential which depends on the occupied state wavefunctions. Thus extra perturbation terms arise from variation of the wave functions ( $\psi$  and  $\psi^*$ ) from the self-consistent potential. The result is (Brown, 1970)

$$(\epsilon_m - \epsilon_i) C_{mi} + \sum_{j,n} [(V_{jm,ni} - V_{jm,in}) C_{nj} + (V_{mn,ij} - V_{mn,ji}) C_{nj}^*] = \omega (J_x)_{mi} \quad (65)$$

and its complex conjugate. The naive perturbation result would be obtained by omitting the terms containing  $V$ . If these terms are omitted, it is easily seen that the Inglis cranking formula follows.

The constrained variation requires the solution of

$$(\sum h_\alpha - \omega J_x) \phi = E_\omega \phi. \quad (66)$$

From second-order perturbation theory using as basis states  $|i\rangle$ ,

$$\sum h_\alpha |i\rangle = \epsilon_i |i\rangle \quad (67)$$

it follows that

$$E_\omega = \sum \epsilon_i - \omega^2 \sum_{i,n} \frac{|(J_x)_{in}|^2}{\epsilon_n - \epsilon_i}. \quad (68)$$

But the nuclear energy is

$$\begin{aligned} E_I &= \langle \phi | \sum h_\alpha | \phi \rangle = E_\omega + \omega \langle \phi | J_x | \phi \rangle \\ &= \sum \epsilon_i + \omega^2 \sum_{i,n} \frac{|(J_x)_{in}|^2}{\epsilon_n - \epsilon_i}, \end{aligned} \quad (69)$$

which is equivalent to Eq. (37c), the cranking result.

The extra terms of Eq. (65) correspond to the fact that the nucleus must be allowed to respond self-consistently to the perturbation caused by the rotation. Without a serious calculation it is difficult to estimate the relative size of the terms containing  $V$  and the primary perturbation term on the right side of Eq. (65), but the importance of the nuclear spectrum is clear.

The similarity between Eq. (65), the linear inhomogeneous equation for the perturbation amplitudes, and the linear homogeneous equations whose solution gives the random phase approximation (RPA) amplitudes is no accident. In fact the use of the usual perturbation formulas, but with Tamm-Dancoff Approximation (TDA) eigenstates and energies as basis states essentially corresponds to the inclusion of the  $V \times C$  term of Eq. (65) while the use of RPA states and energies is equivalent to the full Eq. (65) with both  $V \times C$  and  $V \times C^*$ . Thus these self-consistent corrections to the cranking formula will be important if the residual nuclear interactions are such as to greatly alter the energy and matrix element of  $(1+)$  states connected to  $\phi_0$  by the  $J_x$  operator from their Hartree-Fock values.

For velocity-independent forces, it is shown that this self-consistent correction to the cranking formula comes entirely from the exchange part of the interaction.

It is also shown that the same results can be derived from the time-dependent Hartree-Fock (TDHF) equations. In addition the formalism is readily extended to include pairing correlations by use of the extended Hartree-Fock or Hartree-Fock-Bogoliubov (HFB) method, thus justifying the results of Griffin and Rich (1960) and Nilssen and Prior (1961) to the extent that self-consistent effects of the type described above can be ignored. The additional terms due to the particle-particle and hole-hole parts of the force have recently been calculated and indeed give a small total effect (Meyer, Speth, and Vogler, 1972).

The Peierls-Yoccoz (1957) projection method can also be made to give the correct pushing result by making the projection to good angular momentum before performing the variation of Eq. (58) with respect to the unprojected wave functions. (Zeh, 1965; Rauhanejad and Yoccoz, 1966; Kamlah, 1968; Onishi, 1968).

It was also shown that some corrections to the Belyaev formula [Eq. (56)] are required in a properly invariant self-consistent perturbation treatment of the pairing part of the problem (Katz, 1961; Katz and Blatt, 1961; Prange, 1961). As before, the "pushing" problem was used as a guide to the correct formulation, which is analogous to a gauge invariant treatment of the Meissner effect. Although the original Belyaev formalism gives the wrong answer for the mass in the "pushing" problem, it can be formally brought into agreement (Belyaev, 1961) with the correct Migdal form, and the numerical difference is small.

### G. The Mottelson-Valatin Effect (Detailed Calculation)

The decrease to zero of the pairing gap  $\Delta$  with increasing angular velocity (Mottelson-Valatin CAP effect) was first discussed at length in lectures by Valatin (1962).

#### 1. Perturbation Calculations for Low Spin States

An extensive program of calculations was undertaken by Marshalek (1965, 1967). In these papers the effects of rotation on the pairing gap, on the extent of deformation, and on the quasi-particle motion are all considered. The pairing plus quadrupole model (Bés and Sorensen, 1969) is used for the calculation. In order to obtain the change of moment of inertia with angular velocity Marshalek derived the appropriate expressions for the self-consistent perturbation of the HFB (Hartree-Fock-Bogoliubov with pairing) equations beyond first order in the wave functions and second order in the energy required for the usual cranking type of formula. With  $-\omega J_x$  as perturbation he carried out the calculation self-consistently to fourth order in the energy.

Thus, in an expansion of the type

$$E = AI(I+1) + B[I(I+1)]^2 + C[I(I+1)]^3 + \dots, \quad (70)$$

he determines  $A$  and  $B$ , while in

$$g = g_0 + b\omega^2 + c\omega^4 + \dots \quad (71)$$

$g_0$  and  $b$  would be determined. Since in this calculation all quantities e.g.,  $\Delta$ , etc. are expanded in powers of the angular velocity  $\omega$ , the method is not suitable for studying the large angular momentum region for which the gap has changed from its  $\omega=0$  value all the way down to zero. The rotation must be slow enough that all nuclear properties have changed only a little.

In the calculation, the usual approximations to the pairing plus quadrupole two-body force model are made; namely,

- (1) The quadrupole force contribution to the pairing potentials is ignored, and
- (2) The exchange contribution of the quadrupole force to the self-consistent deformed field is ignored

With these approximations,  $\mathcal{G}_0$  of Eq. (71) and thus  $A$  of Eq. (70) is given by the Belyaev formula [Eq. (56)]. In particular, the self-consistent field corrections from Eq. (65) vanish since the exchange contribution of the quadrupole force is ignored, and also the self-consistent deformed field is essentially of the Nilsson type so  $\mathcal{G}_0$  is as calculated in (Griffin and Rich, 1960; Nilsson and Prior, 1961) except for some parameter adjustments.

The results of the calculation are expressed in terms of the  $B$  parameter of Eq. (70). The calculated (and experimental)  $B$  values are negative corresponding to a positive  $b$  in Eq. (71) or a moment of inertia increasing with increasing angular velocity, as expected from either the CAP effect or from a centrifugal stretching effect.

The calculations indicate that for the well deformed nuclei of the rare earth and actinide regions, the centrifugal stretching effect, due to an increasing self-consistent deformation with rotation, is only a small fraction of the total effect changing the moment of inertia. Only for the lightest rare-earth nuclei is the stretching important.

The calculated ( $-B$ ) parameters for the actinide nuclei agree reasonably well with the experimental values as determined from the  $0+$ ,  $2+$ ,  $4+$ , or  $0+$ ,  $2+$ ,  $4+$ , and  $6+$  level energies, while the calculated values for the well deformed rare-earth nuclei are about a factor of two too large. The calculated  $B$  values have about equal contributions from two sources. The first arises from extending the ordinary independent quasiparticle cranking model as Belyaev did to fourth order in  $\omega$  keeping the deformation and gap parameters  $\Delta$  fixed. The second comes from the change in  $\Delta$  with angular velocity, i.e., the CAP effect in perturbation theory. Similar calculations have been made by Ma and Rasmussen (1970).

The same formalism was also used by Marshalek (1968) to compute the isomer shift, the change of RMS nuclear radius of the rotational  $2+$  state compared to the  $0+$  ground state. For rare-earth nuclei the  $2+$  state is a little larger than the ground state of order  $\Delta R/R \sim 10^{-5}$ . The shifts for the transition nuclei (light Sm and Gd) are larger, and in a few cases for heavier nuclei small negative shifts are observed. The calculated shifts are the right order of magnitude, but tend to be too large by a factor of 2-3. While the main causes of the change in moment of inertia are the Coriolis quasiparticle effect and the CAP effect, the change in radius comes mainly from the centrifugal stretching effect. Recent calculations including hexadecapole  $\beta_4$  deformations give good agreement with experiment (Sano and Wakai, 1972).

## 2. Calculations for High Spin States

The first detailed calculations of the CAP effect valid up to the high spin at which  $\Delta$  goes to zero were made

by Chan and Valatin (1964, 1966). They were followed by a number of increasingly sophisticated but basically similar calculations by various authors (Sano and Wakai, 1965, 1967, 1972; Chan, 1966; Udegawa and Sheline, 1966; Bés, 1968; Krumlinde, 1968, 1971; Ring, Beck, and Mang, 1970; Wakai, 1970; Kumar, 1972).

The idea of these calculations is that the self-consistency regarding the pairing gap and the deformation magnitude should be treated exactly, that is, no power series expansion is assumed for  $\Delta(\omega)$ . The deformation and gap to be selected are those which minimize the energy for fixed expectation of the angular momentum. But the calculation of the energy for fixed deformation and energy gap is done by treating  $-\omega J_Z$  in second order perturbation theory, leading to Eq. (56) for the moment of inertia. This procedure may be valid even for an angular momentum large enough to destroy the pairing gap as long as the energy from  $-\omega J_Z$  is small compared with the quasiparticle excitation energy of the HFB equations. The pairing plus quadrupole force model with the usual approximations has been used in all the calculations for heavy nuclei.

The calculation made by Krumlinde, his method A, can be described as follows: The energy consists of a rotational part involving the usual Belyaev moment of inertia expression [Eq. (56)] and an intrinsic part which also depends on the pairing and quadrupole deformations  $\beta$  and  $\Delta$ . The total energy  $E(\beta, \Delta, I)$  is then minimized for each  $I$  by varying  $\beta$  and  $\Delta$  where

$$E(\beta, \Delta, I) = [I(I+1)/2\mathcal{G}(\beta, \Delta)] + \sum_v 2\epsilon_v V_v^2 - G(\sum_v U_v V_v)^2 - G \sum_v V_v^4 + E_{\text{Coulomb}}(\beta) + (G \sum_v U_v V_v - \Delta) \left( -\frac{1}{2} \frac{I(I+1)}{\mathcal{G}^2} \frac{\partial \mathcal{G}}{\partial \Delta} \right) + \left( \frac{2}{3} \pi \langle Y_{20} \rangle - \beta \right) \left( -\frac{1}{2} \frac{I(I+1)}{\mathcal{G}^2} \frac{\partial \mathcal{G}}{\partial \beta} \right). \quad (72)$$

The first term is the rotational energy, and the next four terms the usual intrinsic energy in the presence of pairing and the Coulomb energy. The last two terms take account of the fact that the moment of inertia should be calculated for the deformations of the particles rather than those of the fields. It is easy to show that minimization of Eq. (72) leads to the modified pairing gap equation of Chan and Valatin (1966), namely:

$$2/G = \sum E_v^{-1} + \omega^2 (\partial \mathcal{G} / \partial \Delta^2). \quad (73)$$

Calculations have been done in which  $\Delta_p$ ,  $\Delta_n$ ,  $\beta_2$ , and  $\beta_4$  have all been varied.

The calculations of Bés *et al.* (1968) and Krumlinde's (1968) method B neglect the last two terms of Eq. (72), and the calculations of Kumar (1972) attempt a better treatment of the self-consistency problem.

One weakness of these calculations is that while they



TABLE II. Critical angular momenta for rare-earth nuclei for the neutron and proton CAP effect from Sano and Wakai (1972).

Nucleus	$A$	$I_c^n$	$I_c^p$
Sm	152	22	40
	154	22	36
Gd	154	22	44
	156	18	42
	158	18	42
	160	14	42
Dy	156	32	46
	158	28	42
	160	18	34
	162	14	32
	164	18	32
E	160	32	44
	162	24	36
	164	16	32
	166	20	32
	168	22	30
	170	12	28
Yb	164	30	36
	166	20	28
	168	24	26
	170	22	32
	172	12	30
	174	16	28
	176	16	20
Hf	170	16	36
	172	18	36
	174	12	34
	176	14	38
	178	12	28
	180	12	24
W	172	22	50
	174	22	48
	176	18	42
	178	14	40
	180	10	38
	182	10	32
	184	18	28
	186	18	30

do include the Coriolis antipairing CAP effect and the centrifugal stretching effects to all orders in  $\omega J_x$ , they treat the direct effect on the quasiparticle only to second order, although Marshalek (1965, 1967) found that at small angular momentum the fourth order effect on the quasiparticles was comparable to the CAP effect. Thus the low spin results of these calculations is certainly suspect. It may be, however, that at high spins, where the Coriolis antipairing is clearly a large effect, the higher order quasiparticle effect may be small enough to be ignored.

Chan and Valatin showed that at increasing spins the gap parameters become smaller and then go suddenly to zero. Further, they found (as confirmed by all the other authors) that the neutron gap goes to zero at a lower spin than does the proton gap. If the  $A$ ,  $B$ , and  $C$  coefficients of Eq. (70) are fitted from the low spin application of the theory, agreement with experiment for  $A$  is good to about  $\pm 15\%$  as previously mentioned. For  $B$  the agreement is also rather good, to about  $\pm 40\%$  for the rare-earth nuclei. Of course that agreement may be fortuitous since it is the omission of Marshalek's quasiparticle contribution that cuts down the value to about the correct size. The  $C$  coefficient is in error by an order of magnitude compared with the experimental result.

The critical angular momentum  $I_c$  at which the neutron pairing vanishes is somewhat higher than the original estimate of Mottelson and Valatin. Table II (Sano and Wakai, 1972) shows that the values of  $I_c$  range from as low as 12 to as high as 32 in the rare-earth region. Krumlinde (1971) who included hexadecapole, quadrupole, and pairing deformations finds less variation with  $16 \gtrsim I_c \gtrsim 20$  for nearly all rare-earth nuclei and  $20 < I_c < 25$  for actinides.

Although changes in deformation usually have a small effect on the energy at low spin, there are cases in the calculations which include deformation effects, in which significant increases in deformation occur at higher spin. At low spin when the pairing is still important the shell effects are somewhat smoothed, and the energy as a function of deformation is a smooth curve with one minimum at the equilibrium deformation. At higher spins the pairing decreases, the shell effects become more pronounced, and the energy as a function of deformation may take on more structure as, for example, by developing two minima with a barrier between them.

As the spin increases the larger deformation becomes more stable relative to the smaller, so that at some value of angular velocity the nucleus may make a sudden transition to a larger deformation and thus to a larger moment of inertia. Such effects are seen in some cases in the calculations of Sano and Wakai and also of Krumlinde. Such a sudden increase in the moment of inertia might produce a discontinuity in the ground-state rotational band much like that caused by the disappearance of pairing.

One interesting result of the fact that the neutron pairing vanishes before that of the protons is that the gyromagnetic ratio factor  $g_R$  for states of the ground-state band should be a decreasing function of spin up to  $I_c$ . The experimental value of  $g_R$  for the  $2+$  states is a little less than  $Z/A$ , the value expected for a rotation of the neutrons and protons together. The reason it is less than  $Z/A$  is because the proton pairing and thus the proton slipping during rotation (giving the reduction in moment of inertia from the rigid value) is



a little larger than that of the neutrons. Thus the charge to mass current ratio under rotation is a little less than  $Z/A$  (Nilsson and Prior, 1961).

As the rotation is increased the pairing decreases, particularly for the neutrons up to spin  $I_c$ . Thus the excess of proton pairing (and slippage) over that of the neutrons increases and  $g_R$  decreases accordingly until at  $I_c$  the neutrons are rotating rigidly and contributing their rigid value to the moment of inertia while the protons are still paired and not rotating as much. At higher spins yet the protons become unpaired and rotate rigidly so that the  $g_R$  factor should rise again to the simple value  $g_R=Z/A$ . Sano and Wakai show a curve for  $^{164}\text{Er}$  for which  $g_R$  drops from about 0.3 to about 0.1 at  $I=18$  and then rises again.

Kumar finds other interesting changes occurring at the angular momentum at which the neutron pairing is dropping rapidly to zero. So much moment of inertia increase is caused by the drop of neutron pairing that it is favorable for the nucleus at the same spins (16–18 for  $^{160}\text{Dy}$ ) to both increase its proton pairing and decrease its deformation with increasing angular momentum to partially offset the effect of the neutron pairing. Unfortunately, it will be very difficult in the near future to measure experimentally the magnetism, deformations, and pairing of the high spin states.

As mentioned earlier, however, the  $B(E2)$  values for the high spin transitions have been determined in one case (see Table I in Sec. IIB2). It is interesting to estimate whether the  $\sim 30\%$  decrease in  $B(E2)$  observed in the backbending region can be reasonably explained on the basis of the CAP effect of a reduction in neutron pairing gap.

If two neighboring spin states  $I, I-2$  have different gap parameters  $\Delta$  and  $\Delta'$ , the corresponding transition should be retarded by the square of the overlap integral

$$R = |\langle \text{BCS}(\Delta) | \text{BCS}(\Delta') \rangle|^2.$$

The overlap integral

$$\langle \text{BCS}(\Delta) | \text{BCS}(\Delta') \rangle = \Pi(U_i U_i' + V_i V_i')$$

is easily calculated for a model with uniformly spaced single-pair degenerate levels of an energy density corresponding to the rare-earth region (three levels per MeV). The result shown in Table III is for 20 levels, but changing to 30 levels makes no difference.

From the experimental data it is clear that the "phase transition" to  $\Delta=0$  is not completely sharp, but takes place over several angular momentum units even in the sharply backbending cases. This may be due to the finite number of particles involved. Although it is not yet possible to calculate in detail the shape of the S curves from microscopic theory as will be discussed in the next sections, the  $\Delta$  value for each spin may be roughly estimated from the energy data. To make the simplest possible estimate for the S-shaped

TABLE III. Overlap integrals  $\langle \text{BCS}(\Delta) | \text{BCS}(\Delta') \rangle$  for 20 levels with 3 levels per MeV, and 20 particles.

$\Delta \backslash \Delta'$	0.0	0.1	0.2	0.3	0.4	0.5
0.0	1.00	0.91	0.76	0.64	0.54	0.46
0.1		1.00	0.96	0.88	0.79	0.72
0.2			1.00	0.98	0.93	0.87
0.3				1.00	0.99	0.95
0.4					1.00	0.99
0.5						1.00

curves, assume that the moment of inertia  $\mathcal{J}$  at spin  $I$  is to be taken from the plots of Fig. 6 by averaging the  $I, I-2$  and the  $I+2, I$  points. Then assume that  $\mathcal{J}(\Delta)$  is a linear function of  $\Delta$  with  $\Delta=0$  at  $\mathcal{J}_{\text{maximum}}$  and  $\Delta=0.8$  MeV for  $\mathcal{J}_0$  the moment of inertia at  $I=0$ . This estimate gives for  $^{168}\text{Er}$   $\Delta=0, 0.09, 0.28, 0.46$  MeV for  $I=16, 14, 12, 10$ , respectively. Table III may then be used to determine that the  $I=16-14$  and  $I=12-10$  transitions should be retarded by about 10–15%, and the  $I=14-12$  transition should be retarded by 20–30% relative to the higher and lower ones, in reasonable agreement with the experimental results (Ward *et al.*, 1973). A similar estimate for the smoother  $^{168}\text{Dy}$  suggests retardation of only about 10% at most. These rough estimates should not be taken too seriously as they include only one effect, but they may give the order of magnitude of the expected effect.

Work has continued in efforts to justify a higher order cranking model since for heavy nuclei at high spins any other type of treatment is still too involved calculationally (Marshalek and Weneser, 1969, 1970). A number of other fundamental discussions of rotation have been presented (Klein and Kerman, 1965; Klein *et al.*, 1968; Onishi and Yoshida, 1966; Kammuri, 1967; Belyaev and Zelevinskii, 1970).

### 3. The Shape of the Singular Behavior at High Spin

Because of the recent experiments showing a sudden rise in moment of inertia at about spin 16 and the suggestion that this is indeed the Mottelson–Valatin CAP effect, there is renewed interest in determining in more detail the predicted shape of the ground-state band in the vicinity of the singularity.

The CAP calculations indicate a moment of inertia which rises with increasing angular momentum until the neutron gap vanishes at which point the moment of inertia stops at a value corresponding to the rigid moment (for the neutrons). It would be expected to rise again until the proton gap vanishes and then remain at the full rigid value. In the calculations using the BCS formalism a discontinuity in the slope of the  $\mathcal{J}$  vs  $I$  curve will occur when  $\Delta_n=0$ . Since  $\mathcal{J}=I/\omega=I/(dE/dI)$ , such a discontinuity implies only a discontinuity in the second derivative of the  $E$  vs  $I$  curve. Since the data

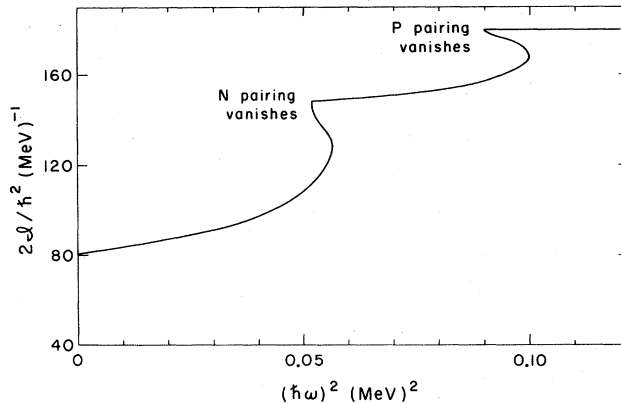


FIG. 7. The first  $\mathcal{J}$  vs  $\omega^2$  curve as inferred from graphs of Chan and Valatin (1964, 1966).

are for discrete  $I$  values it would be difficult to prove the existence or nonexistence of that discontinuity from experiment.

In fact, this discontinuity at  $\Delta=0$  is an artificial feature of the BCS approximation associated with the failure to require conservation of the number of particles. Many suggestions have been made concerning exact and approximate number projection schemes to improve the BCS equations. [See for example Ref. 27 of Bés and Sorensen (1969).] A particularly simple method (Sorensen, 1972) was suggested by the author. Instead of the usual BCS wave function

$$\psi_I = \prod_j (U_j + V_j a_j^\dagger a_j^\dagger) |0\rangle, \quad (74)$$

the wave function

$$\psi = \prod_j (U_j + V_j a_j^\dagger a_j^\dagger) |0\rangle \pm \prod_j (U_j - V_j a_j^\dagger a_j^\dagger) |0\rangle \quad (75)$$

is used as a trial function. While  $|\text{BCS}\rangle$  Eq. (74) contains all numbers of pairs, Eq. (75) contains only even/odd numbers of pairs of particles. This gives a much improved energy, especially near  $\Delta=0$ , and eliminates the singularity in the second derivative of  $E_0$  vs  $G$ , where  $E_0$  is the ground-state energy of a pairing force with strength  $G$  (this singularity is closely related to the  $E$  vs  $I$  singularity just discussed). This method is used for discussion of the moment of inertia by Sorensen (1971).

It is also used in recent calculations by Faessler *et al.* (1972). Calculations have been made for rotational levels to high spin (8+) in Light nuclei (Satpathy and Nair, 1968; Beck *et al.*, 1970; Gunze and Khadkikar, 1970; Sandhya *et al.*, 1970; Goeke and Faessler, 1971; Goeke *et al.*, 1972; Grin and Leinson, 1972; Marshalek, 1972; Parikh, 1972). These are not cranking calculations, but use a wave function of the Hartree-Fock-Bogoliubov type projected to definite angular mo-

mentum. "Realistic" forces have also been used rather than the schematic pairing plus quadrupole type. These calculations with the projection to definite angular momentum made before that variation which determines the pairing correlation give rather good results for  $s$ ,  $d$  shell nuclei and show an antipairing effect with increasing spin.

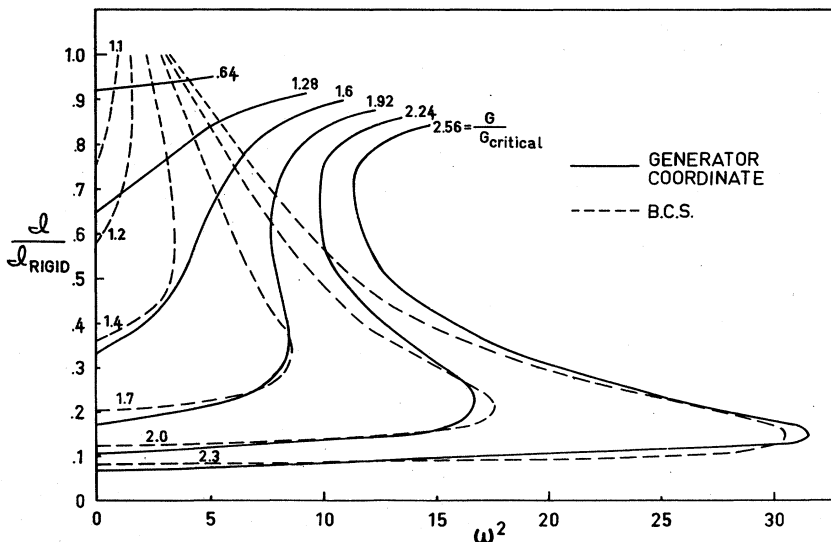
Similar calculations using the pairing plus quadrupole force model have now been reported for the rare-earth nuclei  $^{160}\text{Dy}$  and  $^{162}\text{Er}$  (Faessler *et al.*, 1973). The number projection is done using the simple method described above. The angular momentum projection to high spin requires a fine mesh of integration points and is still only feasible if the deformations are restricted to being axial. In the calculations reported, only one gap parameter is varied, the other quantities (e.g., the deformation parameter  $\beta$ ) being held fixed at some appropriate value. The calculations, with parameters chosen to fit the low-frequency part of the spectrum, do resemble the experimental results at high spin. However, it is not clear that very good results should be expected from such a calculation based on a projection of the small components of high spin from an HFB wave function with zero expectation value for this spin. For heavy well-deformed nuclei, the high spin rotating state may look very little like the high spin component of a nonrotating axially deformed state.

#### 4. The S-Shaped Curves

While the existence or nonexistence of a discontinuity in the second derivative of  $E$  vs  $I$  might be difficult to verify, the fact that in some cases (eight to date) the moment of inertia rises so rapidly with angular momentum that the angular frequency  $\omega = I/\mathcal{J}$  decreases momentarily is easily seen in the data, and appears as an S-shaped curve in the  $\mathcal{J}$  vs  $\omega^2$  plot. This backbending occurs in the work of Chan and Valatin as seen in Fig. 7, and in the subsequent work and depends on the strength of the pairing force and the distribution of single-particle levels. In particular, the stronger the pairing force relative to the critical value at which pairing just begins, the stronger is the backbending tendency due to the CAP effect. Such backbending for a schematic two-level cranking model with pairing is shown in Fig. 8.

While the experimental backbending is certainly real enough, none of the microscopic calculations performed so far can be trusted in this backbending region. As long as the backbending is not too sharp (only one  $\omega$  for each angular momentum) all portions of the curve should correspond to rotations stable against small oscillations in the moment of inertia. Thus, the picture of the nucleus as having a reasonably sharp angular velocity as well as sharp angular momentum right through the points on the S portion of the curve may be correct.

FIG. 8. Curves of  $\mathcal{I}$  vs  $\omega^2$  as a function of the strength of the pairing force for the two-level model.  $G$  critical is the minimum pairing force strength at which there is pairing at  $\omega=0$  in the BCS approximation. The two levels each have pair degeneracy  $\Omega=8$ . The dashed curve uses the equations of Krumlinde's (1968) method A while the solid curves use an improved pairing approximation (Sorensen, 1971). Only the pairing degree of freedom is considered.



So the cranking model of the nucleus, with particles moving in a rotating deformed potential and having pairing interactions, may be able to give a satisfactory description of the spectrum. This is much more difficult than the usual pairing problem since the one-body force, with the Coriolis term  $-\omega j_x$  included, has eigenstates none of which are time reverse pairs. With the use of these one-body eigenstates as basis states, the pairing force has the usual pairing matrix elements connecting pairs in states which were time reverse pairs at  $\omega=0$ , but with a reduced, state dependent coupling constant  $G_{\text{eff}} < G$ . In addition there are new off-diagonal matrix elements for pairs of particles in pairs of states which do not become time reverse pairs at  $\omega=0$ .

The original estimate of  $I$  critical of Mottelson and Valatin (1960) ignored the off-diagonal terms which tend to push  $I$  critical to somewhat higher values. The more recent calculations include both the usual reduced pairing terms and the off-diagonal terms in an approximate way. All of these calculations involve a perturbation treatment of the angular velocity  $\omega$  at some stage, e.g., in the calculation of the one-body states and energies, and the calculation of the effective pairing force parameters. An exact diagonalization of the HFB equations in the presence of the Coriolis force has not yet been presented. A cranked HFB calculation projected to definite angular momentum and definite number of particles is still more difficult.

The cranking model as it has been used for heavy nuclei only requires the expectation value for angular momentum to be fixed. For a backbending  $\mathcal{I}$  vs  $\omega^2$  curve, the  $E$  vs  $I$  curve (the yrast line) has an indentation or concave downward portion as in Fig. 2 since the decreasing  $\omega$  corresponds to a decreasing slope. The cranking procedure minimizes the energy, with the

angular momentum constraint, for a certain class of wave functions, namely HFB functions. But, an exact solution of the cranking problem (minimize  $\langle H \rangle$  for fixed  $I = \langle j_x \rangle$ ) must follow a curve like the dashed line of Fig. 2 and would thus have no backbending. A state of good angular momentum  $I$  on the solid curve in the backbending region can be changed so as to lower its energy expectation while still retaining  $I$  for  $\langle j_x \rangle$ . This will be the case if the state is changed to a linear combination of a good  $I$  state from the top and one from the bottom of the dashed line of Fig. 2. The exact cranking procedure without angular momentum projection thus eliminates backbending by producing a variational wave function with a large angular momentum spread. Thus backbending obtained in unprojected approximate cranking procedures must be considered spurious or at least unreliable.

It is possible to imagine cases in which  $V$  of Eqs. (6-9) is so irregular that some intermediate values of  $\mathcal{I}$  between  $\mathcal{I}_0$  and  $\mathcal{I}_{\text{max}}$  are unstable so that the  $\mathcal{I}$  vs  $\omega^2$  curve would actually have a break or a missing section. But at each angular momentum  $I$ , there will be a state of lowest energy. Thus missing angular momentum states as discussed by Sano, Takemasa, and Wakai (1972) must be a spurious result owing to the use of an inadequate variational wave function.

For a believable microscopic calculation avoiding spurious singularities, the wave function must have both the correct angular velocity (cranking), and the right angular momentum (projection), and the right number of particles to a degree of approximation thus far unavailable for calculation of heavy nuclei. But it may be that the difficult angular momentum projection can be accomplished (for a cranked wave function, which already has the correct average angular momentum) with sufficient accuracy by the use of just a

few wave functions in analogy to the scheme described for approximately projecting the particle number in Eq. (75). Other approximate projection techniques have been discussed recently (Bishari, 1971; Lee and Cusson, 1972; Pradhan *et al.*, 1972; Ullah, 1972).

It has also been suggested that the angular momentum may be sharpened by including extra constraint conditions, e.g.,  $\langle J^2 \rangle$ ,  $\langle J^3 \rangle$  etc., in addition to the cranking constraint that  $\langle J_x \rangle = I$  (Wahlborn, 1972). An algebraic method for calculations in a  $j$  shell model has been given by Vallieres *et al.* (1972).

### 5. Tri-Axial Nuclei

Another weakness of the microscopic calculations made to date is that only axially symmetric deformations have been considered. While at low spin well-deformed nuclei are mostly axial, at very high spin they are almost certain to be tri-axial. It is easy to see that the centrifugal force on a nucleus rotating about an axis perpendicular to its symmetry axis will be such as to try to increase the moment of inertia about the rotation axis. Likewise the Coriolis force on individual orbits in the rotating nucleus acts to tilt or deform the orbit so that the particle angular momentum points toward the direction of rotation. This also acts to make the nucleus tri-axial.

Bohr (1970) and Mottelson (1971) have suggested that above  $I \approx 20$  the character of the low levels may be that of an asymmetric rotor. Such a motion is suggested as a possible explanation of the several tracks of transitions required to explain the termination of the line spectrum at  $I = 20$ . The yrast line at these high spins would correspond to rotation about the nuclear axis with the largest moment of inertia. Other tracks will occur parallel to and with small equidistant spacings above the yrast line, corresponding to rotations with the rotation axis tilted in small steps away from the largest moment of inertia axis. These higher tracks correspond classically to motions with increasing amounts of wobble of the symmetry axis.

Solutions of the tri-axial rotor problem show selection rules enhancing gamma transitions along one of these tracks over transitions across tracks down to the yrast line (the lowest track). Thus different nuclei of the ensemble will follow different tracks, rather than all going at once to the yrast line at high spin and producing the unobserved lines.

### 6. State-Dependent Energy Gap

All the microscopic theories used so far describe the pairing correlation in terms of a single parameter such as  $\Delta$  the pairing gap, which is driven to zero by the Coriolis coupling. In contrast, the detailed rotor plus valence calculations of Stevens and Simon (1972), referred to later as SS, suggest that the first "singular" effect of the rotation is to decouple only a single high

spin pair of particles. The microscopic theory can neither confirm nor deny that idea unless the microscopic wave function used has enough freedom to choose whether just one pair shall first be decoupled or whether the entire paired nucleus will move to the normal nonsuperconducting state. Such a decoupling of one pair at a time has been suggested by Birbrair (1971, 1972) to be the consequence of the nuclear Meissner effect. Explicit predictions are made that the decoupling should occur at the lowest spin values for  $N = 90$  and  $N = 112(110)$  in no particular agreement with the experimental results.

## V. PARTICLES PLUS ROTOR MODELS

To avoid the delicate and difficult problems of self-consistency discussed at length in the preceding section, there have been several calculations of the high spin states using a model of several particles coupled to an axial rotor whose only degree of freedom is its rotation.

In these calculations the particles mutually interact with two-body forces, and also with the rotor in such a way as to conserve the total rotor plus particle angular momentum. Thus both the self-consistency and angular momentum projection problems are eliminated in the model, but at considerable expense in believability. If, in the model, the number of particles is small (two or four), the unchanging parameterized rotor may be a reasonable approximation, but many-body effects will be absent or mistreated. On the other hand, if the number of particles is large (the last oscillator shell or two) then the many-body effects may be well represented, but it is unreasonable that the rotor not change its deformation and/or pairing in the presence of a significant change of the particle wave function. Another weakness of the theory is that  $\mathcal{J}$  at  $I = 0$  cannot really be calculated since the rotor moment of inertia  $\mathcal{J}_R$  is an ad hoc parameter.

### A. Krumlinde-Szymanski (KS) Calculation

However, within the model, the calculations can and have been done in reasonable detail and with good accuracy. Krumlinde and Szymanski (1971, 1972, 1972a) have exactly solved the rotor plus particles model for a particularly simple schematic case with the use of group theory.

The Hamiltonian is the sum of rotor kinetic energy  $T$  and the particle Hamiltonian  $H_p$ , which is described in terms of the intrinsic coordinate system tied to the rotor. The total angular momentum  $I$  is the sum of the rotor  $R$  and particle  $j_x$  angular momenta. For two dimensions (rotations about the  $x$  axis perpendicular to the symmetry axis  $z$ ) the total Hamiltonian is

$$H = (I - j_x)^2 / (2\mathcal{J}_R) + H_p, \quad (76)$$

where the first term is the rotor kinetic energy. The

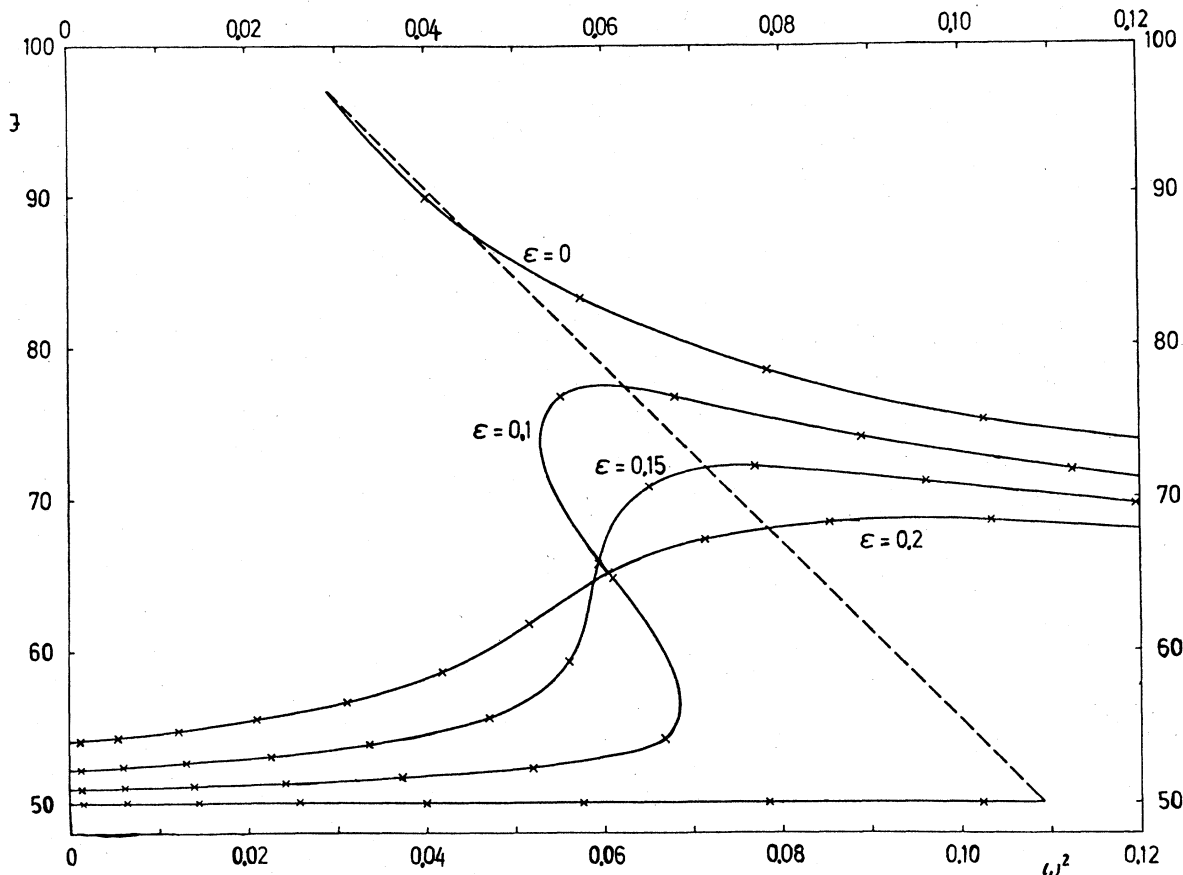


FIG. 9. Curves of  $g$  vs  $\omega^2$  as calculated by Krumlinde and Szymanski (1971) for the two-level plus rotor model. The different curves correspond to different ratios of the pairing force strength to the single-particle splitting,  $\epsilon$ .

intrinsic particle Hamiltonian  $H_p$  is taken to be the sum of two terms  $H_{sp}$  and  $H_{pair}$ . The single-particle part  $H_{sp}$  is taken to be just two multiply degenerate levels looking, for example, like a set of  $\Omega = \pm 13/2$  doubly degenerate Nilsson-type states all at one energy, and an equal set of  $\Omega = \pm 11/2$  states at another energy. The  $j_x$  operator is assumed to connect each state at the one energy with one state at the other energy with a state-independent matrix element. The two-body force  $H_{pair}$  is the usual pairing force which has a constant matrix element connecting a  $\pm\Omega$  pair from one of the energy levels with every other  $\pm\Omega$  pair from that level or from the other energy level.

The problem represented by the Hamiltonian Eq. (76) is then solved exactly with results similar to those previously described. While  $I = R + j_x$  is a constant of the motion and is thus simply a  $c$  number in Eq. (76),  $j_x$  is not, and the resultant states are not eigenstates of  $j_x$ .

For  $I=0$ , the ground state will have  $\langle j_x \rangle = 0$ . For  $I > 0$ , the ground-state wave function will change in order to reduce the rotational energy somewhat by

making  $\langle j_x \rangle$  positive. When  $I$  is very large, the particles will be completely aligned to maximum  $j_x$  with no pairing correlations remaining, and further increases in  $I$  will just increase the rotational energy with no change of the particle wave function.

Thus for large  $I$  from Eq. (76) we have

$$E_I = (I - j_x)^2 / (2g_R) + C, \quad (77)$$

where  $j_x$  and  $C$  are constants. Then from Eqs. (4) and (5) we can calculate

$$\omega = (I - j_x) / g_R \quad (78)$$

and

$$g = I / \omega = [I / (I - j_x)] g_R. \quad (79)$$

Thus, for large  $I$  the moment of inertia decreases toward  $g_R$  of the rotor with increasing  $I$  or  $\omega$ . If the pairing is strong compared with the energy splitting of the two single-particle levels, we have  $j_x = 0$ , and a good quantum number for the low  $I$  states, and the  $I=0$  moment of inertia is also  $g_R$ . That is, the particles are superfluid and make no contribution to  $g$ . For weaker

pairing (compared to the single-particle splitting)  $j_x$  is not a good quantum number, and at low  $I$ , the energy  $E_I$  increases more slowly with  $I$  since  $\langle j_x \rangle$  can change a little, decreasing the rotational energy. This corresponds to  $\mathcal{J} > \mathcal{J}_R$  at  $I=0$  so the particles are contributing to the moment of inertia.

Thus  $\mathcal{J}$  starts at or above  $\mathcal{J}_R$  at  $I=0$ , increases to a maximum, and then decreases with increasing  $I$  or  $\omega$  back to the value  $\mathcal{J}_R$  of the rotor alone. In the case of strong pairing, the increase of  $\mathcal{J}$  is sudden, leading to an S-shaped curve of  $\mathcal{J}$  vs  $\omega^2$ , while for weaker pairing (or larger single-particle level splitting) the rise is smoother with no backbending of the  $\mathcal{J}$  vs  $\omega^2$  curve as shown in Fig. 9. The curves clearly resemble the experimental ones, and this is not changed by the extension to three dimensions or the inclusion of more than two single-particle levels (Krumlinde and Szymanski, 1972) although both complicate the calculation. Whether or not it will be practical to solve the equations for a "realistic" set of single-particle Nilsson-like levels remains to be seen.

### B. Stephens-Simon Calculation

The calculations of Stephens and Simon (1972) have essentially the same physical starting point as those just described, namely, they are based on the three-dimensional version of Eq. (76). From that starting point, the calculations diverge in a number of ways.

Krumlinde and Szymanski (KS) treat exactly a schematic  $H_p$  while Stephens and Simon (SS) attempt an approximate treatment of a realistic  $H_p$ . In the SS calculation  $H_p$  is a reasonable Nilsson one-body potential with pairing, and particular attention is paid to levels originating from the neutron  $i 13/2$  level since these have the largest Coriolis matrix elements and would appear to be important in the rare earth region. The pairing is treated in the quasiparticle approximation with fixed occupation parameters with only zero and two quasiparticle states included in most cases (inclusion of four quasiparticle states in a somewhat restricted space did not make important changes for  $I < 20$ ). This approximate treatment of pairing precludes the possibility of describing the Mottelson-Valatin effect except to the extent that the two quasiparticle state describes reduced pairing. The unpaired wave function would require many quasiparticles of a paired basis for its description, if the pairing is strong.

Thus in SS it is emphasized that a new phenomenon (not the Mottelson-Valatin CAP effect) is being discussed, namely, a decoupling of one  $i 13/2$  neutron pair from the rotating core.

The rotor is also treated differently in the two cases. While KS use a fixed  $\mathcal{J}_R$  for the rotor and thus make a clean separation between rotor and particle degrees of freedom, SS adds realism by allowing the rotor moment of inertia  $\mathcal{J}_R$  to depend on the state of the particles. In

particular, for two quasiparticle matrix elements  $\mathcal{J}_R$  was taken to be about 15% larger than for zero to zero or for zero to two quasiparticle matrix elements, to simulate the fact that pairing is somewhat reduced in the two quasiparticle state yielding a larger expected moment of inertia. At this point, of course, it becomes somewhat unclear just how many particles are supposed to be represented by the core and how many by the quasiparticles.

Both KS and SS exactly diagonalize the resulting Eq. (76), KS by using the group theory necessary since the particle space is large; and SS by using direct matrix diagonalization with realistic  $j_x$  matrix elements from Nilsson states, which is possible since the particle space is restricted to a small number of degrees of freedom.

The result of the SS calculation is that the Coriolis force from the cross term of the rotational energy in Eq. (76)

$$H_c = - (I/\mathcal{J}_R) \cdot j_x \quad (80)$$

[compare with the term  $-\omega L_x$  of Eq. (41)] has the effect of tilting the  $i 13/2$  particles orbits so that they tend to point their angular momentum in the direction of the rotor angular momentum. This tendency of the Coriolis force to align the particle angular momenta in the direction of the rotation, thus breaking the zero angular momentum pairing, is the origin of the CAP effect, but the SS wave functions allow only one pair to be broken or decoupled. A related decoupled picture has recently been observed by Stephens *et al.* (1972) in some odd nuclei.

It is observed by SS that for the lighter rare-earth nuclei, for which  $i 13/2$  contains only a few particles, the nuclear force due to the deformed potential favors the lowest  $\Omega$  values (projection of particle angular momentum on the nuclear symmetry axis) for a prolate deformation, and the highest  $\Omega$  values for an oblate deformation. The Coriolis force favors the orbit which has its angular momentum in the rotor angular momentum direction, perpendicular to the nuclear symmetry axis. This state is made up predominately of states of low  $\Omega$ . Thus for the actual case of prolate deformations in the light rare earths, the tilted orbits favored by the Coriolis force are not strongly disfavored by the nuclear force, and the pair of  $i=13/2$  particles may be decoupled at relatively low spin values.

For the heavy rare-earth nuclei for which the  $i 13/2$  orbit is nearly filled, the same argument shows that only if the nuclei were oblate, could the pair be broken at low spin values. Thus since the heavy rare earths are, in fact, prolate, it is expected that the decoupling of a pair at low spin will occur only for the light rare-earth nuclei and not for the heavy ones.

With the use of "realistic" parameter values, SS obtain results resembling the experiments in the vicinity of the singular region near  $I=16$ . Their transition is

essentially one from the lower moment of inertia of the no quasiparticle ground-state band at lower spins to the higher moment of inertia of the two quasiparticle band (which comes below the no quasiparticle band for  $I \gtrsim 16$ ) at higher spins. It should be noted, however, that for parameters chosen to fit the S-shaped moment of inertia vs  $\omega^2$  curves, the curve near  $\omega \approx 0$  is much more nearly constant than the experimental values, whose moments of inertia show a sizeable linear term in the  $\mathcal{J}$  vs  $\omega^2$  plot. Thus this theory does not account for the wave function changes occurring at low spin.

The main feature distinguishing the SS calculation from all the rest is its prediction that the singularity for the heavy rare-earth nuclei will occur, if at all, at much higher spin values than that of the light rare-earth nuclei. This is in disagreement with the recent data from Michigan (Warner and Bernthal, 1972) which shows sudden increases in  $\mathcal{J}$  for  $N=106$  nuclei. It does seem clear that, for  $N=98$ , the band is smoother at high spin than it is for lower neutron numbers, in agreement with SS. Whether or not this would be in agreement with the CAP picture is not clear.

Concerning other properties, the SS model and the CAP picture predict remarkably similar results. For example, the CAP effect predicts a decreasing  $g$  value with increasing spin, and so does the SS picture since, as the  $i$  13/2 neutrons decouple, they make their contribution to the moment; and the  $g$  factor for  $i$  13/2 neutrons is negative, thus subtracting from the positive ( $Z/A$ ) value of the rotor.

The  $B(E2)$  values for transitions  $I, I-2$  near the singular (or band crossing) point are found in the SS model to be only a little reduced (less than 10%) from the rotational value. This is also in agreement with the new data on  $^{168}\text{Er}$  (Ward *et al.*, 1973a).

The similarity between the SS results and those of the CAP effect is not so surprising since the difference between those two pictures is not as great as might appear at first sight. In the SS picture, the singular behavior occurs upon the breaking of one pair of neutrons, while in CAP, as described in the BCS approximation with a state-independent gap parameter, it occurs when the pairing correlations are completely destroyed for all the neutrons.

But the pairing in deformed nuclei is not very strong, so that the number of neutrons whose wave functions are changed by the pairing correlations is rather small in the first place. A measure of the total pair degeneracy close enough to the Fermi surface to be affected by the correlations is  $\Delta/G$ , where  $\Delta$  and  $G$  are the pairing gap and force strength. The number of pairs involved in the correlations is about half this number. Using typical values of  $G=0.13$  and  $\Delta=0.65$ , this indicates that there are only two or three extra pairs due to the pairing force, so that the loss of one pair as in the SS picture goes a long way toward the complete destruc-

tion of the pairing correlations. In both pictures it is the neutrons which become unpaired first.

The long-range mass number dependence of the CAP effect may be different from that of the single-pair decoupling (Sheline, 1972). He predicts that while the CAP effect is most important (has the smallest  $I$  critical value) for lighter nuclei, the single-pair decoupling will come first for the actinides. The two effects, if distinct, are competing in the rare-earth region.

## VI. CONCLUSIONS

The rotational states to high spin give a unique opportunity for the study of the response of a nucleus to an almost continuously variable disturbance over a wide range of strength, namely the Coriolis and centrifugal forces. The sudden change in the spectrum at  $I \approx 16$  shows that a small change in the "force" is making a large change in the wave function at that point.

The origin of the effect is semiquantitatively understood as a competition between the pairing force, which prefers pairs of like particles near the Fermi surface to have opposite angular momenta ( $j^2$ ) <sub>$J=0$</sub> , and the Coriolis force, which breaks the time reversal  $jm, j-m$  degeneracy of the single-particle states, thus reducing the pairing, and prefers particles near the Fermi surface to be aligned with their angular momenta pointed in the rotation direction. The importance of the Coriolis antipairing CAP effect is clear, but the precise nature of the singularity producing the observed sudden rise in moment of inertia is not yet convincingly established. It is not clear, for example, whether the BCS pairs are all broken at once, or one at a time; whether the change to nonaxial shape of the nucleus is important; or whether sudden changes in nuclear deformation occur so as to modify significantly the basic picture. Before such questions can be answered more difficult calculations must be performed.

Additional experimental information would also be of great value. In addition to the extension in the  $N, Z$  plane of the detailed knowledge of high spin states of the yrast line, some information on the second (and higher) state of given high spin near the singularity would be particularly useful. Since a small change in Coriolis force causes a large wave function change, there must be a near instability near the critical angular momentum. This implies that the first excited spin 14 state must be close in energy to the lowest  $I=14$  state. If the origin of the singular behavior at  $I \approx 14$  is indeed the CAP effect, the excited state should be of the nature of a pairing vibration state which appears as a low excitation whenever the pairing gap is about to be lost.

No evidence is seen for such states above the yrast line in the ( $HI, xn$ ) experiments in which the ground

band is populated at the top.<sup>2</sup> It is possible, however, that in multiple Coulomb excitation experiments near or just above the Coulomb barrier, such states might be populated from below as the spin rises. The energy favoring of decays to the yrast line, present in the ( $HI$ ,  $xn$ ) case, do not play such a dominant role in coulomb excitation and furthermore there is the possibility of a direct two particle transfer occurring at high spin. In this way, direct evidence concerning the

character of the change occurring at the critical angular momentum could, in principle, be obtained.

#### ACKNOWLEDGMENTS

During the course of preparation of this review I had the pleasure of seeing preprint versions of related material by Johnson and Szymanski (1972a) and by Kumar (1972a). I wish to acknowledge many helpful discussions particularly with S. Wahlborn, Z. Szymanski, and the experimentalists at the Research Institute for Physics during my stay there supported in part by NORDITA, and also with L. Wolfenstein. Preparation of the article was supported by the National Science Foundation.

<sup>2</sup> An exception has just been presented by D. Ward, H. R. Andrews, J. S. Geiger, and R. L. Graham (1973b) in which levels of <sup>166</sup>Dy are observed in ( $\alpha$ ,  $3n$ ) and (<sup>12</sup>C,  $4n$ ). The data are interpreted as a "crossing" of the ground and beta bands at  $I \approx 16$  and the two  $I \approx 16$  states are only about 25 keV apart in energy.

- Amado, R. D., and K. A. Brueckner, 1959, Phys. Rev. **115**, 778.  
 Bardeen, J., L. N. Cooper, and J. R. Schrieffer, 1957, Phys. Rev. **108**, 1175.  
 Beck, R., H. J. Mang, and P. Ring, 1970, Z. Phys. **231**, 26.  
 Belyaev, S. T., 1959, K. Dan. Vidensk. Selsk. Mat.-Fys. Medd. **31** (11).  
 Belyaev, S. T., 1961, Nucl. Phys. **24**, 322.  
 Belyaev, S. T., and V. G. Zelevinskii, 1970, Sov. J. Nucl. Phys. **11**, 416.  
 Bés D., S. Landowne, and M. A. J. Mariscotti, 1968, Phys. Rev. **166**, 1045.  
 Bés D., and R. A. Sorensen, 1969, Adv. Nucl. Phys. **2**, 129.  
 Birbrair, B. L., 1971, Phys. Lett. B **34B**, 558.  
 Birbrair, B. L., 1972, Phys. Lett. B **39B**, 489.  
 Bishari, M., I. Unna, and A. Mann, 1971, Phys. Rev. C **3**, 1715.  
 Bogoliubov, N. N., 1958, Zh. Eksp. Teor. Fiz. **34**, 58.  
 Bogoliubov, N. N., 1958a, Zh. Eksp. Teor. Fiz. **34**, 73.  
 Bogoliubov, N. N., 1958b, Nuovo Cimento **7**, 794.  
 Bohr, A., 1970, "Symmetry Properties of Nuclei," XV ème Conseil International de Physique, Bruxelles, Belgique, Sept. 1970.  
 Bohr, A., and B. Mottelson, 1955, K. Dan. Vidensk. Selsk. Mat.-Fys. Medd. **30** (1).  
 Brown, G., 1964, *Unified Theory of Nuclear Models* (North-Holland, Amsterdam), p. 69 (1964).  
 Brown, G., 1970, in *Facets of Physics*, edited by A. Bromley and V. Hughes (Academic, New York), p. 141 (1970).  
 Buescher, H., W. F. Davison, R. M. Lieder, and C. Mayer-Böricke, 1972, Phys. Lett. B **40B**, 449.  
 Chan, K. Y., 1966, Nucl. Phys. **85**, 261.  
 Chan, K. Y., and J. G. Valatin, 1966a, Nucl. Phys. **82**, 222.  
 Chan, K. Y., and J. G. Valatin, 1964, Phys. Lett. **11**, 304.  
 Corben, H. C., and P. Stehle, 1950, *Classical Mechanics* (Wiley, New York), p. 182 (1950).  
 Diamond, R. M., F. S. Stephens, and W. J. Swiatecka, 1964, Phys. Lett. **11**, 315.  
 Diamond, R. M., F. S. Stephens, W. H. Kelly, and D. Ward, 1969, Phys. Rev. Lett. **22**, 546.  
 Draper, J. E., 1972, Phys. Lett. B **41B**, 105.  
 Faessler, A., L. Lin, and F. Wittmann, 1972, abstract, Conference on High Spin Nuclear States and Related Phenomena, Stockholm (May 1972).  
 Faessler, A., L. Lin, and F. Wittman, 1973, Phys. Lett. B **44B**, 127.  
 Goeke, K., and A. Faessler, 1971, Phys. Lett. B **35B**, 289.  
 Goeke, K., A. Faessler, and H. H. Wolter, 1972, Nucl. Phys. **A183**, 352.  
 Goeke, K., H. Muther, and A. Faessler, 1973, preprint (1973).  
 Griffin, J. J., and J. A. Wheeler, 1957, Phys. Rev. **108**, 311.  
 Griffin, J. J., and M. Rich, 1960, Phys. Rev. **118**, 850.  
 Grin, Yu. T., and L. B. Leinson, 1972, Yad. Fiz. **14**, 55.  
 Gross, E. P., 1959, Nucl. Phys. **14**, 389.  
 Gunze, M. R., and S. B. Khadkikar, 1970, Phys. Rev. Lett. **24**, 910.  
 Gupta, R. K., 1971, Phys. Lett. B **36B**, 173.  
 Harris, S. M., 1965, Phys. Rev. **138B**, 509.  
 Hill, D. L., and J. A. Wheeler, 1953, Phys. Rev. **89**, 1102.  
 Inglis, D. R., 1954, Phys. Rev. **96**, 1059.  
 Inglis, D. R., 1956, Phys. Rev. **103**, 1786.  
 Johnson, A., H. Ryde, and J. Starkier, 1971, Phys. Lett. B **34B**, 605.  
 Johnson, A., H. Ryde, and S. A. Hjorth, 1972, Nucl. Phys. A. **A179**, 753.  
 Johnson, A., and Z. Szymanski, 1973, Phys. Rpts. **7C**, 181.  
 Kamlah, A., 1968, Z. Phys. **216**, 52.  
 Kammuri, T., 1967, Prog. Theor. Phys. **37**, 1131.  
 Katz., A., 1961, Nucl. Phys. **26**, 129.  
 Katz., A. and J. Blatt, 1961, Nucl. Phys. **23**, 612.  
 Klein, A., and A. K. Kerman, 1965, Phys. Rev. **138**, B1323.  
 Klein, A., M. Dreizler, and R. E. Johnson, 1968, Phys. Rev. **171**, 1216.  
 Krumlinde, J., 1968, Nucl. Phys. **A121**, 306.  
 Krumlinde, J., 1971, Nucl. Phys. **A160**, 471.  
 Krumlinde, J., and Z. Szymanski, 1971, Phys. Lett. B **36B**, 157.  
 Krumlinde, J., and Z. Szymanski, 1972, Phys. Lett. B **40B**, 314.  
 Krumlinde, J., and Z. Szymanski, 1972a, abstract, Conference on High Spin Nuclear States and Related Phenomena, Stockholm, (May 1972).  
 Kumar, K., 1972, Abstract, Conference on High Spin Nuclear States and Related Phenomena, Stockholm (May 1972).  
 Kumar, K., 1972a, Physica Scripta **6**, 270.  
 Lark, N. L., and H. Morinaga, 1965, Nucl. Phys. **63**, 466.  
 Lee, H. C., and R. Y. Cusson, 1972, Phys. Lett. B **39B**, 453.  
 Lieder, R. M., H. Beuscher, W. F. Davidson, P. Jahn, H.-J. Probst, and C. Mayer-Böricke, 1972, Phys. Lett. B. **39B**, 196.  
 Ma, C. W., and J. O. Rasmussen, 1970, Phys. Rev. C **2**, 798.  
 Mariscotti, M. A. J., G. Scharff-Goldhaber, and B. Buck, 1969, Phys. Rev. **178**, 1869.  
 Mariscotti, M. A. J., 1970, Phys. Rev. Lett. **24**, 1242.  
 Marshalek, E. R., 1965, Phys. Rev. **139**, B770.  
 Marshalek, E. R., 1967, Phys. Rev. **158**, 993.  
 Marshalek, E. R., 1968, Phys. Rev. Lett. **20**, 214.  
 Marshalek, E. R., 1972, Phys. Lett. B **38B**, 367.  
 Marshalek, E. R., and J. Weneser, 1969, Ann. Phys. (N.Y.) **53**, 569.  
 Marshalek, E. R., and J. Weneser, 1970, Phys. Rev. C **2**, 1682.  
 Meyer, J., J. Speth, and J. H. Vogler, 1972, Nucl. Phys. **A193**, 60.  
 Meyer, J., J. Speth, and J. H. Vogler, 1973, preprint (1973).  
 Migdal, A. B., 1959, Nucl. Phys. **13**, 655.  
 Migdal, A. B., 1959a, Sov. Phys.-JETP **37**, 249.  
 Molinari, A., and T. Regge, 1972, Phys. Lett. B **41B**, 93.



- Morinaga, H., and P. C. Gugelot, 1963, Nucl. Phys. **46**, 210.  
 Morinaga, H., and N. L. Lark, 1965, Nucl. Phys. **67**, 315.  
 Moszkowski, S. A., 1956, Phys. Rev. **103**, 1328.  
 Mottelson, B. R., 1962, Selected Topics in the Theory of Collective Phenomena in Nuclei, in *Nuclear Spectroscopy*, edited by G. Racah (Academic, New York, 1962).  
 Mottelson, B. R., 1971, Rotational Motion in the Nucleus in *The Nuclear Structure Symposium of the Thousand Lakes*, Jyväskylä, Finland (June 1971).  
 Mottelson, B. R., and S. G. Nilsson, 1959, K. Dan. Vidensk. Selsk. Mat.-Fys. Medd. **1** (8).  
 Mottelson, B. R., and J. G. Valatin, 1960, Phys. Rev. Lett. **5**, 511.  
 Newton, J. O. et al., 1970, Nucl. Phys. **A141**, 631.  
 Nilsson, S. G., 1955, K. Dan. Vidensk. Selsk. Mat.-Fys. Medd. **29** (16).  
 Nilsson, S. G., and O. Prior, 1961, K. Dan. Vidensk. Selsk. Mat.-Fys. Medd. **32** (16).  
 Nordhagen, R., G. Goldring, R. M. Diamond, K. Nakai, and F. S. Stephens, 1970, Nucl. Phys. **A142**, 577.  
 Onishi, N., 1968, Prog. Theor. Phys. **40**, 84.  
 Onishi, N., and S. Yoshida, 1966, Nucl. Phys. **80**, 367.  
 Parikh, J. K., 1972, Phys. Rev. C **5**, 153.  
 Peierls, R. E., and D. J. Thouless, 1962, Nucl. Phys. **38**, 154.  
 Peierls, R. E., and J. Yoccoz, 1957, Proc. Phys. Soc. Lond. A **A70**, 381.  
 Pradham, H. C., Y. Nogami, and J. Law, 1973, Nucl. Phys. **A201**, 357.  
 Prange, R. E., 1961, Nucl. Phys. **22**, 283.  
 Ring, P., R. Beck, and H. J. Mang, 1970, Z. Phys. **231**, 10.  
 Rockmore, R. M., 1959, Phys. Rev. **116**, 469.  
 Rockmore, R. M., 1960, Phys. Rev. **118**, 1645.  
 Rauhanejad, H. and J. Yoccoz, 1966, Nucl. Phys. **78**, 353.  
 Saethre, O., 1973, S. A. Hjorth, A. Johnson, S. Jägere, H. Ryde, and Z. Szymanski, preprint (1973).  
 Sandhya Devi, K. R., S. B. Khadkikar, J. K. Parikh, and B. Banerjee, 1970, Phys. Lett. B **32B**, 179.  
 Sano, M., T. Takemasa, and M. Wakai, 1973, preprint (1973).  
 Sano, M., and M. Wakai, 1965, Nucl. Phys. **67**, 481.  
 Sano, M., and M. Wakai, 1967, Nucl. Phys. **A97**, 298.  
 Sano, M. and M. Wakai, 1972, Prog. Theor. Phys. **47**, 880.  
 Sano, N. and M. Wakai, 1972a, preprint (1972).  
 Satpathy, L., and S. C. K. Nair, 1968, Phys. Lett. B **26B**, 257.  
 Satpathy, L., and L. Satpathy, 1971, Phys. Lett. B **34B**, 377.  
 Scharff-Goldhaber, G., and A. S. Goldhaber, 1970, Phys. Rev. Lett. **24**, 1349.  
 Sheline, R. K., 1972, preprint (1972).  
 Sorensen, R. A., 1971, "Variation of the Moment of Inertia with Angular Velocity in the Two-Level Model," in *Colloque sur les Noyaux de Transition*, 30 Juin 1971, Institut de Physique Nucléaire d'Orsay (1971).  
 Sorensen, R. A., 1972, Phys. Lett. B **38B**, 376.  
 Stephens, F. S., N. L. Lark, and R. M. Diamond, 1964, Phys. Rev. Lett. **12**, 225.  
 Stephens, F. S., N. L. Lark, and R. M. Diamond, 1965, Nucl. Phys. **63**, 82.  
 Stephens, F. S., and R. S. Simon, 1972, Nucl. Phys. **A138**, 257.  
 Stephens, F. S., R. M. Diamond, J. R. Leigh, T. Kammuri, and K. Nakai, 1972, Phys. Rev. Lett. **29**, 438.  
 Sunyar, A. W., 1972 abstract, Conference on High Spin Nuclear States and Related Phenomena, Stockholm (May 1972).  
 Sunyar A. W., O. C. Kistner, E. der Matsosian, P. Thieberger, A. H. Lumpkin, and C. Cochavi, 1972a, Bull. Am. Phys. Soc. **17**, 913.  
 Taras, P., W. Dehnhardt, S. J. Mills, M. Veggian, J. C. Merdinger, U. Neumann, and B. Povh, 1972, Phys. Lett. B **41B**, 295.  
 Thieberger, P., A. W. Sunyar, P. C. Rogers, N. Lark, O. C. Kistner, E. der Mateosian, S. C. Cochavi, and E. A. Auerbach, 1972, Phys. Rev. Lett. **28**, 972.  
 Thieberger, P., 1973, preprint (1973).  
 Thouless, D. J., 1960, Nucl. Phys. **21**, 225.  
 Thouless, D. J., and J. G. Valatin, 1960, Phys. Rev. Lett. **5**, 509.  
 Thouless, D. J., and J. G. Valatin, 1962, Nucl. Phys. **31**, 211.  
 Trainor, L. E. H., and R. K. Gupta, 1971, Can. J. Phys. **49**, 133.  
 Udagawa, T., and R. K. Sheline, 1966, Phys. Rev. **147**, 671.  
 Ullah, N., 1972, Phys. Rev. C **5**, 285.  
 Valatin, J. G., 1956, Proc. R. Soc. A **A238**, 132.  
 Valatin, J. G., 1958, Nuovo Cimento **7**, 843.  
 Valatin, J. G., 1961, "Superconducting Electron and Nucleon Systems" in *Lectures in Theoretical Physics*, Boulder, Colorado, 1961 (Interscience, New York, 1962), Vol. IV, p. 1 (1961).  
 Vallieres, M., A. Klein, and R. M. Dreizler, 1972, Phys. Lett. B **41B**, 125.  
 Villars, F., 1957, Annu. Rev. Nucl. Sci. **7**, 211.  
 Wahlborn, S., 1972, abstract, Conference on High Spin States in Nuclei and Related Phenomena, Stockholm (May 1972).  
 Wahlborn, S., and R. K. Gupta, 1972, Phys. Lett. B **40B**, 27.  
 Wakai, M., 1970, Nucl. Phys. **A141**, 423.  
 Ward, D., F. S. Stephens, and J. O. Newton, 1967, Phys. Rev. Lett. **19**, 1247.  
 Ward, D., H. R., Andrews, J. S. Geiger, R. L. Graham, and J. F. Sharpey-Schaefer, 1973a, Phys. Rev. Lett. **30**, 493.  
 Ward, D., H. R. Andrews, J. S. Geiger, and R. L. Graham, 1973b, preprint and Bull. Am. Phys. Soc. **18**, 630.  
 Warner, R. A., and F. M. Bernthal, 1972, Bull. Am. Phys. Soc. **17**, 899.  
 Wick, G. C., 1948, Phys. Rev. **73**, 51.  
 Yoccoz, J. 1957, Proc. Phys. Soc. Lond. A **A70**, 388.  
 Zeh, H. D., 1965, Z. Phys. **188**, 361.